Dalton Transactions

PAPER

View Article Online
View Journal | View Issue

Cite this: *Dalton Trans.*, 2015, **44**, 14159

Synthesis and characterisation of halide, separated ion pair, and hydride cyclopentadienyl iron bis(diphenylphosphino)ethane derivatives†

Dipti Patel,[a] Ashley Wooles,[a] Andrew D. Cornish,[a] Lindsey Steven,[a] E. Stephen Davies,[a] David J. Evans,*[b] Jonathan McMaster,[a] William Lewis,[a] Alexander J. Blake[a] and Stephen T. Liddle*[a]

Received 16th February 2015,
Accepted 7th July 2015

DOI: 10.1039/c5dt00704f

www.rsc.org/dalton

Treatment of anhydrous FeX_2 (X = Cl, Br, I) with one equivalent of bis(diphenylphosphino)ethane (dppe) in refluxing THF afforded analytically pure white (X = Cl), light green (X = Br), and yellow (X = I) $[FeX_2(dppe)]_n$ (X = Cl, **I**; Br, **II**; I, **III**). Complexes **I–III** are excellent synthons from which to prepare a range of cyclopentadienyl derivatives. Specifically, treatment of **I–III** with alkali metal salts of C_5H_5 (Cp, series **1**), C_5Me_5 (Cp*, series **2**), $C_5H_4SiMe_3$ (Cp′, series **3**), $C_5H_3(SiMe_3)_2$ (Cp′′, series **4**), and $C_5H_3(Bu^t)_2$ (Cp^{tt}, series **5**) afforded $[Fe(Cp^{\dagger})(Cl)(dppe)]$ **1Cl–5Cl**, $[Fe(Cp^{\dagger})(Br)(dppe)]$ **1Br–5Br**, and $[Fe(Cp^{\dagger})(I)(dppe)]$ **1I–5I** ($Cp^{\dagger}$ = Cp, Cp*, Cp′, Cp′′, or Cp^{tt}). Dissolution of **1I–5I** in acetonitrile, or treatment of **1Cl–5Cl** with Me_3SiI in acetonitrile (no halide exchange reactions were observed in other solvents) afforded the separated ion pair complexes $[Fe(Cp^{\dagger})(NCMe)(dppe)][I]$ **1SIP–5SIP**. Attempts to reduce **1Cl–5Cl**, **1Br–5Br**, and **1I–5I** with a variety of reductants (Li-Cs, KC_8, Na/Hg) were unsuccessful. Treatment of **1Cl–5Cl** with $LiAlH_4$ gave the hydride derivatives $[Fe(Cp^{\dagger})(H)(dppe)]$ **1H–5H**. This report provides a systematic account of reliable methods of preparing these complexes which may find utility in molecular wire and metal–metal bond chemistries. The complexes reported herein have been characterised by X-ray diffraction, NMR, IR, UV/Vis, and Mössbauer spectroscopies, cyclic voltammetry, density functional theory calculations, and elemental analyses, which have enabled us to elucidate the electronic structure of the complexes and probe the variation of iron redox properties as a function of varying the cyclopentadienyl or halide ligand.

Introduction

One of the most popular and widely used organometallic transition metal anions in the literature is $[FeCp(CO)_2]^-$ (Fp^-).[1] The Fp^- anion has been used extensively in nucleophilic displacement reactions and in the preparation of metal–metal bonds.[2] Regarding the latter point, although the nucleophilicity of the Fp anion should favour M–Fe bond formation, there is a significant possibility of iso-carbonyl bond formation with early, electropositive and oxophilic metals,[3] an area which we have been investigating in recent years.[4] One approach to avoid iso-carbonyl bridges is to employ cyclopentadienyl iron fragments that are supported by two monodentate or one bidentate phosphine ligand[s]. This approach has enabled the isolation of a range of novel linkages and has also been implemented in rare earth-ruthenium chemistry.[5]

Recently, we reported four uranium–ruthenium bonds using the ruthenium analogue of Fp.[6] As part of that study we found that the corresponding uranium–iron (Fp) linkages could not be isolated. We reasoned that substitution of the carbonyl groups with phosphines might increase the steric protection and thus stability of uranium–iron linkages which would necessitate the preparation of the corresponding iron precursors. Since substitution of the carbonyl groups *in situ* is not feasible, it would be necessary to start with a cyclopentadienyl–phosphine ligand set before constructing the uranium–iron bond.

Two methods of preparing uranium–iron bonds could be envisaged, either reductive cleavage of a Fe–Fe species, as has been accomplished with cobalt,[10] or protonolysis of a uranium alkyl or amide with an iron hydride.[4] One approach to iron cyclopentadienyl ligand derivatives would be to prepare the relevant iron cyclopentadienyl dicarbonyl halide or hydride

[a]*School of Chemistry, University of Nottingham, University Park, Nottingham, NG7 2RD, UK*
[b]*Department of Chemistry, University of Hull, Hull, HU6 7RX, UK.*
E-mail: stephen.liddle@nottingham.ac.uk, david.evans@hull.ac.uk

†Electronic supplementary information (ESI) available: Electrochemical, DFT, and Mössbauer data for **1Cl–5Cl**, **1Br–5Br**, **1I–5I**, **1SIP–5SIP**, and **1H–5H**, and X-ray data for **I–III**, **1Cl**, **3Cl–5Cl**, **1Br**, **3Br–5Br**, **2I–5I**, **1SIP–5SIP**, and **1H–5H**. CCDC 1049712–1049737. For ESI and crystallographic data in CIF or other electronic format see DOI: 10.1039/c5dt00704f

then substitute the carbonyl with phosphines, but it is known that this approach can be complicated by the formation of mono-substituted complexes,[7] or the formation of chelated derivatives with the retention of one CO ligand and expulsion of the halide ligand from the primary coordination sphere of iron.[8] We therefore decided to prepare phosphine chelated iron(II) halides, introduce the cyclopentadienyl ligand, then either reduce or substitute the halide with hydride. This methodology has been shown to work in a few cases,[7] but the data in the literature are fragmented and sometimes incomplete. In particular, solid state structures are often missing but would provide valuable benchmarking for previously reported spectroscopic and computational studies. Given the importance of cyclopentadienyl iron bis(diphenylphosphino)ethane (dppe) fragments in assembling molecular wires[9] as well as representing synthons to iron–metal bonds it would be desirable to draw together a cohesive and comprehensive description of a reliable general methodology for the preparation of a range of well characterised and understood functionalised iron cyclopentadienyl dppe derivatives where the steric and electronic properties can be systematically varied.

Here, we report the synthesis of three iron(II) halide dppe complexes, and their utility in preparing a range of cyclopentadienyl derivatives. We describe attempts to reduce these cyclopentadienyl dppe halide complexes to the corresponding diiron derivatives, and also the synthesis of hydride congeners. In all, we describe the synthesis of twenty five iron cyclopentadienyl dppe complexes as either halide, separated ion pair, or hydride derivatives which has enabled us, through a structural and spectroscopic benchmarking study, to provide reliable synthetic methods and a detailed understanding of the electronic structure of these compounds. This report thus constitutes a cohesive account of compounds which could find extensive utility in molecular wire and metal–metal bond chemistries.

Results and discussion

Synthesis of iron(II) halide dppe adducts

We began by preparing dppe adducts of iron(II) halides from the reaction between anhydrous FeX_2 (X = Cl, Br, I) and one equivalent of dppe in refluxing THF, Scheme 1. Following filtration, removal of solvent, washing with toluene, and drying, analytically pure white (X = Cl), light green (X = Br), and yellow (X = I) solids were obtained in ~95% yield in each case. It is notable that although these simple coordination complexes $[FeX_2(dppe)]_n$ (X = Cl, **I**; Br, **II**; I, **III**) are often mentioned in the literature,[7] detailed descriptions of their synthesis and characterisation are scant and the structure of **II** is unknown. In all three cases we were able to determine the solid state structures by X-ray crystallography (Fig. 1). The solid state structures of **I** and **III** were determined from crystals grown from THF, for **I**, an infinite polymer is observed in the solid state with tetrahedral iron centres and bridging dppe ligands whereas in **III** a dimer is formed containing two tetrahedral iron centres which are each bridged by two dppe ligands. In contrast, the bromide compound **II** could be isolated as the polymeric (**II**) or dimeric (**IIa**) forms from THF/hexane or toluene solutions, respectively. Langer and co-workers have recently independently found that **I** co-crystallises with $[FeCl_2(dppe)_2]$ from a chloroform/acetone mixture in a polymeric chain similar to our findings, and also solely if the reaction is completed in the correct stoichiometry, with similar bond lengths and angles to those found in **I**.[7] Pohl *et al.* elucidated the solid state structure of $[Fe_2I_2(dppe)_4]$ from toluene solution and also found it to be dimeric in nature, with similar bond lengths and angles to those found in **III** which crystallised from THF solvent,[7] suggesting that the isolation of polymeric or dimeric forms of **I–III** is due to the halide and not solvent effects.

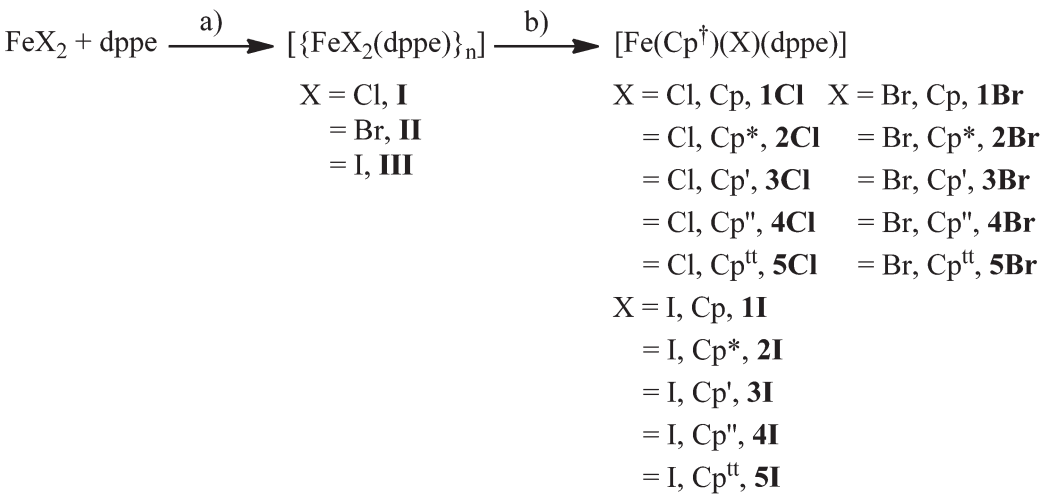

Scheme 1 Synthesis of **I**, **II**, **III**, **1Cl–5Cl**, **1Br–5Br**, **1I–5I**. Reagents and conditions: (a) THF, Δ; (b) LiCp/NaCp/KCp†, toluene, –78 °C, –LiCl/KCl/NaI/KCl/KBr/KI.

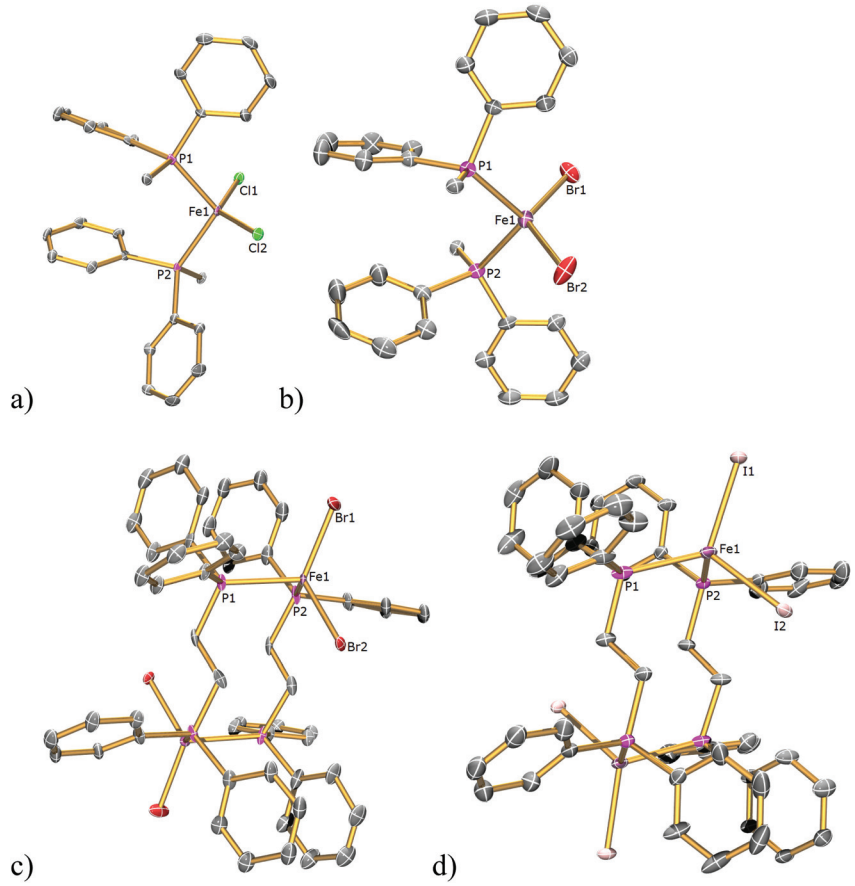

Fig. 1 Solid state asymmetric unit structures of (a) **I** (polymer), (b) **II** (polymer), (c) **IIa** (dimer), (d) **III** (dimer) with ellipsoids set at 40% probability. Hydrogen atoms and minor disorder components are omitted for clarity. Selected bond lengths (Å) and angles (°): (a) Fe1–Cl1 2.2416(16), Fe1–Cl2 2.2403(15), Fe1–P1 2.4422(16), Fe1–P2 2.4849(16), Cl1–Fe1–Cl2 127.14(6), Cl1–Fe1–P1 104.65(6), Cl1–Fe1–P2 100.74(6), Cl2–Fe1–P1 100.80(6), Cl2–Fe1–P2 111.50(6), P1–Fe1–P2 111.80(5); (b) Fe1–Br1 2.368(8), Fe1–Br2 2.370(9), Fe1–P1 2.468(12), Fe1–P2 2.454(13), Br1–Fe1–Br2 121.22(3), Br1–Fe1–P1 100.24(4), Br1–Fe1–P2 114.25(4), Br2–Fe1–P1 108.10(4), Br2–Fe1–P2 105.65(4), P1–Fe1–P2 107.54(4); (c) Fe1–Br1 2.375(2), Fe1–Br2 2.372(2), Fe1–P1 2.429(4), Fe1–P2 2.464(4), Br1–Fe1–Br2 119.38(9), Br1–Fe1–P1 108.77(12), Br1–Fe1–P2 107.56(12), Br2–Fe1–P1 108.65(13), Br2–Fe1–P2 111.71(12), P1–Fe1–P2 98.77(12); (d) Fe1–I1 2.5856(9), Fe1–I2 2.5659(9), Fe1–P1 2.4748(18), Fe1–P2 2.4963(18), I1–Fe1–I2 116.98(3), I1–Fe1–P1 106.75(4), I1–Fe1–P2 110.21(4), I2–Fe1–P1 113.32(5), I2–Fe1–P2 109.30(4), P1–Fe1–P2 99.81(5).

Synthesis and characterisation of halide and separated ion pair complexes

With the synthesis of **I–III** in-hand we first targeted cyclopentadienyl derivatives using C_5H_5 (Cp, series **1**), C_5Me_5 (Cp*, series **2**), $C_5H_4SiMe_3$ (Cp′, series **3**), $C_5H_3(SiMe_3)_2$ (Cp″, series **4**), and $C_5H_3(Bu^t)_2$ (Cp^{tt}, series **5**) since this selection provides a wide variation of steric and electronic (σ-donor, π-acceptor) properties. Thus, treatment of **I–III** with one equivalent of the relevant lithium/sodium/potassium (Cp) or potassium ($Cp^{*/'/''/tt}$) cyclopentadienyl reagent in toluene at −78 °C afforded, after filtration and removal of toluene, generally black solids, Scheme 1. Recrystallisation from toluene or dichloromethane layered with hexane (**1Cl**) afforded the target complexes [Fe(Cp)(Cl)(dppe)] (**1Cl**), [Fe(Cp*)(Cl)(dppe)] (**2Cl**), [Fe(Cp′)(Cl)(dppe)] (**3Cl**), [Fe(Cp″)(Cl)(dppe)] (**4Cl**), [Fe(Cp^{tt})(Cl)(dppe)] (**5Cl**), [Fe(Cp)(Br)(dppe)] (**1Br**), [Fe(Cp*)(Br)(dppe)] (**2Br**), [Fe(Cp′)(Br)(dppe)] (**3Br**), [Fe(Cp″)(Br)(dppe)] (**4Br**), [Fe(Cp^{tt})(Br)(dppe)] (**5Br**), [Fe(Cp)(I)(dppe)] (**1I**), [Fe(Cp*)(I)(dppe)] (**2I**), [Fe(Cp′)(I)(dppe)] (**3I**), [Fe(Cp″)(I)(dppe)] (**4I**), and [Fe(Cp^{tt})(I)(dppe)] (**5I**), in crystalline yields of *ca.* 50–70%. We note that apart from some minor decomposition, the bulk products are fairly pure (*ca.* 90%) and that the crystalline yields principally reflect the solubility of the cyclopentadienyl derivatives. During this work we noted that the temperature of the initial salt elimination reaction is important since the formation of ferrocenes and free dppe from ligand scrambling is a competing side reaction which becomes a major by-product at room temperature. However, ferrocenes formation is suppressed and indeed essentially eliminated if reactions are initially conducted at −78 °C. Compound **1I** can also be prepared from [Fe(CO)$_2$(Cp)]$_2$ with treatment with iodine followed by addition of dppe in refluxing toluene, however in lower yields of 48% compared to the above method in which yields of **1I** reach 67%.[11]

Halide exchange in iron cyclopentadienyl phosphine derivatives has previously been effected by mixing complexes such as

2Cl with, for example, KI,[12] whereas the approach outlined above gives direct access to chloride, bromide, and iodide derivatives. In an attempt to ascertain whether any other methods have applicability here, we screened the reactivity of the chlorides with trimethylsilyl iodide. Interestingly, although **1Cl–5Cl** are inert with respect to halide exchange in THF, toluene, and dichloromethane, in acetonitrile spontaneous displacement of the chloride ligand by acetonitrile and facile halide exchange occurs to afford the separated ion pair (SIP) complexes [Fe(Cp)(NCMe)(dppe)][I] (**1SIP**), [Fe(Cp*)(NCMe)(dppe)][I] (**2SIP**), [Fe(Cp′)(NCMe)(dppe)][I] (**3SIP**), [Fe(Cp″)(NCMe)(dppe)][I] (**4SIP**), and [Fe(Cp^{tt})(NCMe)(dppe)][I] (**5SIP**) as red powders following work-up (Scheme 2). Recrystallisation of these powders from acetonitrile afforded **1SIP–5SIP** in crystalline yields of typically 65–75%, although **3SIP** is a notable outlier (36% crystalline yield). Since SIPs form readily we did not investigate this avenue further with the bromides, but it is germane to note that complexes **1SIP–5SIP** represent valuable precursors to a range of separated ion pair species such as known PF_6-derivatives.

We investigated the reduction of **1Cl–5Cl**, **1Br–5Br**, and **1I–5I** with a variety of reductants (Li-Cs, KC_8, Na/Hg), but in all cases either no reaction occurred, or on extended stirring decomposition was observed. This might be attributed to the iron centres being electron rich, and more so than in Fp because of less effective back-bonding to dppe compared to two CO ligands. This would also be consistent with the relative ease of oxidising these complexes (see below). We therefore focussed on preparing the hydrides.

Synthesis of hydride complexes

With the aforementioned halide complexes in hand we examined their conversion to the corresponding hydrides. Accordingly, treatment of the chloride series **1Cl–5Cl** with 5 equivalents of lithium aluminium hydride in THF afforded, after removal of solvent, extraction into hexane, filtration and removal of solvent, the hydride complexes [Fe(Cp)(H)(dppe)] (**1H**), [Fe(Cp*)(H)(dppe)] (**2H**), [Fe(Cp′)(H)(dppe)] (**3H**), [Fe(Cp″)(H)(dppe)] (**4H**), and [Fe(Cp^{tt})(H)(dppe)] (**5H**) as orange solids that are approximately 90% pure, Scheme 2. Recrystallisation of **1H–5H** from hexane afforded orange crystalline materials in yields typically ranging from 41 to 73%, but, as was the case for the SIP complex **3SIP**, the crystalline yield of the Cp′ and Cp″ derivatives **3H** and **4H** are notably low (35 and 41%, respectively). It should be noted that **3H** and **4H** are far less stable than the other three hydride derivatives and decompose in solution over a few hours, which is, in part, reflected in their crystalline yields. Complexes **1H** and **2H** have been previously reported, however, in the preparation of **1H** an excess of $NaBH_4$ was reacted with the chloroform adduct of **1Cl** giving only a 50% yield[13] and **2H** was reported to have been synthesised by the same method outlined above or alternatively by reacting **I** with Cp*H in a colloidal dispersion of potassium metal in THF; a reaction which reportedly proceeds *via* the formation of a "Fe(dppe)" intermediate followed by oxidative addition of Cp*H.[14]

Solid state structures

The solid-state structures of **1Cl**, **3Cl–5Cl**, **1Br**, **3Br–5Br**, **2I–5I** were determined by single-crystal X-ray diffraction studies and are illustrated in Fig. 2–4, respectively, and key metrical data are presented in Table 1. The structures of **2Cl**[14] and **1I**[15] were determined previously and the experimental data obtained of crystals of **2Br** were of insufficient quality to determine meaningful metrical parameters. Each complex displays a pianostool geometry, and in comparison to the ideal bond angle of a classical tetrahedral geometry of 109.5°, the X1–Fe1–P1, X1–Fe1–P2, P1–Fe1–P2 angles span the ranges 86.03(4)–93.12(2), 84.18(4)–92.12(10) and 80.78(5)–86.22(3)° in **1Cl–5Cl**, **1Br–5Br** and **1I–5I** respectively, due in part to the restrictive bite angle of the dppe ligand but mainly due to the large size of the various substituted Cp ligands forcing the other ligands closer together. This results in large Ct–Fe1–X1, Ct–Fe1–P1, Ct–Fe1–P2 angles ranging 118.97(9)–123.9(9), 126.37(7)–132.6(11) and 124.8(2)–132.98(13)° respectively. The Fe1–Ct bond lengths span the narrow range of 1.699(3)–1.743(12) Å in all of the complexes, which compares well to the Fe–$Cp_{centroid}$ average distance of 1.740 Å in complexes containing both dppe and Cp ligands.[16] The Fe–P bond distances span the narrow range of 2.184(2)–2.2580(9) Å, which compares to Fe–P bond distances in complexes containing both Cp and dppe ligands in the range 2.1168(19)–2.3105(14) Å.[16] The Fe–Cl, Fe–Br, Fe–I distances of 2.294(2)–2.346(1), 2.2464(6)–2.481(3) and 2.643(1)–2.661(2) Å respectively increase as expected according to increasing ion size in the order I > Br > Cl. Although a range of different substituted Cp ligands have been studied and

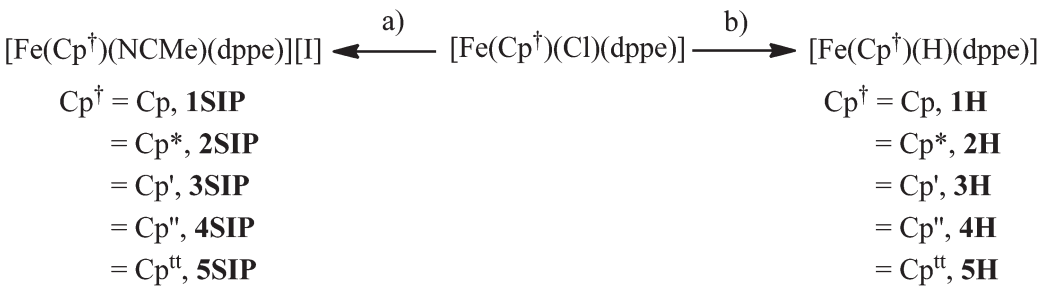

Scheme 2 Synthesis of **1SIP–5SIP**, **1H–5H**. Reagents and conditions: (a) TMSI, MeCN, −TMSCl; (b) excess $LiAlH_4$, THF, −LiCl.

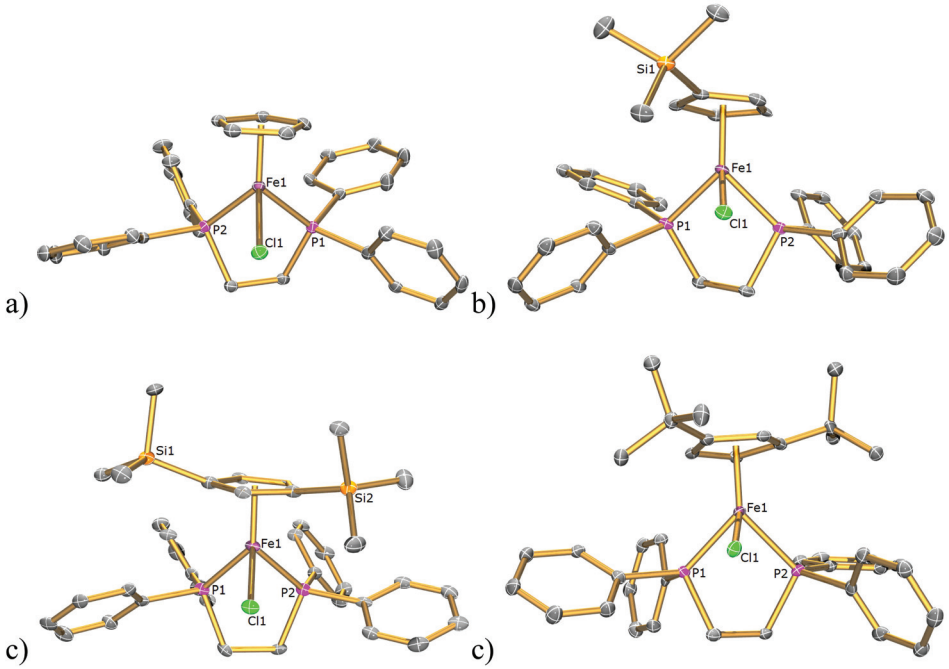

Fig. 2 Solid state structures of (a) **1Cl**, (b) **3Cl**, (c) **4Cl**, (d) **5Cl** with ellipsoids set at 40% probability. Hydrogen atoms are omitted for clarity.

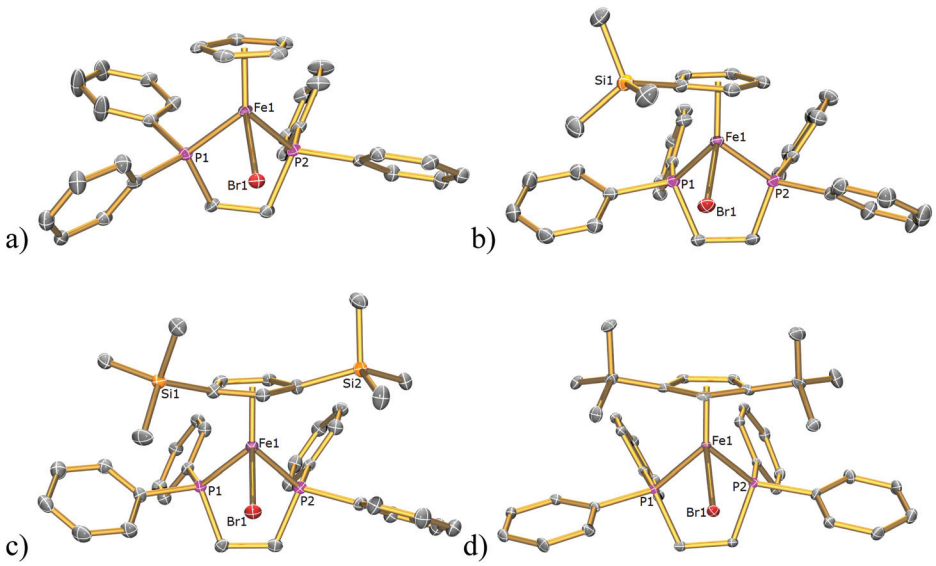

Fig. 3 Solid state structures of (a) **1Br**, (b) **3Br**, (c) **4Br**, (d) **5Br** with ellipsoids set at 40% probability. Hydrogen atoms are omitted for clarity.

characterised the difference in their steric properties appears to have no major effect on the bond angles and lengths of the other ligands.

The solid-state structures of **1SIP–5SIP** were determined by single-crystal X-ray diffraction studies and are illustrated in Fig. 5 with key bond distances listed in Table 1. The geometries of these complexes are similar to those featured in the halide complexes except that an acetonitrile, not a halide, ligand is coordinated to the iron centres. The Fe1–Ct bond lengths range 1.709(4)–1.732(4) Å and are comparable to those found in **1I–5I** (1.707(3)–1.743(12) Å) and the Fe–P bond lengths range from 2.1986(12)–2.247(2) Å and are comparable to those found in **1I–5I** (2.188(1)–2.2580(9) Å. The Fe–N bond lengths range from 1.892(7)–1.908(4) Å and are comparable to those found in the literature with complexes containing dppe and Cp ligands (1.881(5)–1.909(8) Å).[16] The Ct–Fe–N and Ct–Fe–P angles range 120.8(15)–123.4(10) and 124.27(13)–132.27(12)° respectively, and are comparable with the Ct–Fe–I

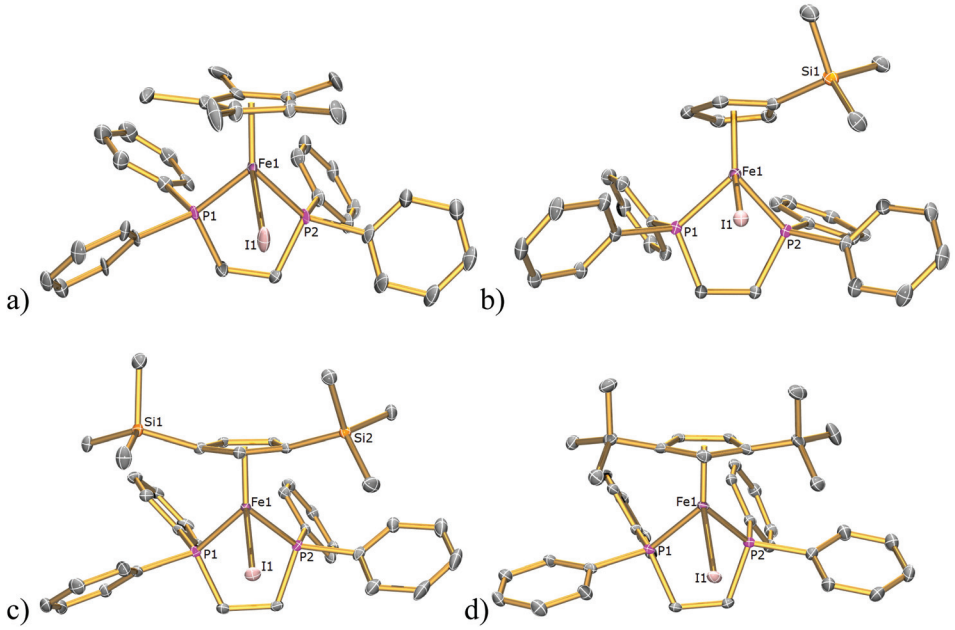

Fig. 4 Solid state structures of (a) **2I**, (b) **3I**, (c) **4I**, (d) **5I** with ellipsoids set at 40% probability. Hydrogen atoms are omitted for clarity.

Table 1 Selected bond lengths (Å) for the new crystal structures **1Cl**, **3Cl–5Cl**, **1Br**, **3Br–5Br**, **2I–5I**, **1SIP–5SIP** and **1H–5H**[a]

Compound	Fe–Ct	Fe–X	Fe1–P1	Fe1–P2
1Cl	1.699(3)	2.3317(9)	2.1963(10)	2.1846(10)
3Cl	1.716(5)	2.3298(16)	2.1980(16)	2.1881(15)
4Cl	1.704(7)	2.294(2)	2.184(2)	2.194(2)
5Cl	1.739(4)	2.3423(10)	2.2107(11)	2.2358(10)
1Br	1.699(5)	2.4647(6)	2.1909(10)	2.1958(10)
3Br	1.709(18)	2.481(3)	2.1909(5)	2.2059(5)
4Br	1.720(5)	2.464(8)	2.201(13)	2.210(13)
5Br	1.734(4)	2.476(8)	2.2273(13)	2.2578(13)
2I	1.743(12)	2.661(2)	2.221(3)	2.208(3)
3I	1.712(2)	2.6478(4)	2.1874(7)	2.1956(7)
4I	1.728(2)	2.6464(4)	2.2018(7)	2.2116(7)
5I	1.734(3)	2.6603(5)	2.2266(10)	2.2580(9)
1SIP	1.713(3)	1.900(2)	2.2188(7)	2.2194(7)
2SIP	1.732(4)	1.896(3)	2.2034(13)	2.2214(11)
3SIP	1.709(4)	1.908(4)	2.1986(12)	2.1940(12)
4SIP	1.730(2)	1.9063(19)	2.2392(7)	2.2429(7)
5SIP	1.727(7)	1.892(7)	2.240(2)	2.247(2)
1H	1.702(4)	1.60(4)	2.1455(1)	2.1292(10)
2H	1.712(7)	1.56(7)	2.1255(18)	2.1448(19)
3H	1.698(3)	1.50(4)	2.1404(9)	2.1196(9)
4H	1.701(5)	1.39(2)	2.1333(13)	2.1302(13)
5H	1.707(8)	1.52(14)	2.142(2)	2.153(2)

[a] Ct = centroid of the cyclopentadienyl ring; X = Cl, Br, I, acetonitrile N or H.

and Ct–Fe–P bond angles of 118.97(7)–123.78(7), 126.37(7)–133.93(4)° respectively found in **1I–5I**. The N–Fe–P and P1–Fe–P2 bond angles of 88.79(10)–93.24(12) and 85.48(4)–86.47(4)° respectively lie within the range shown for the I–Fe–P and P1–Fe–P2 angles in **1I–5I** (88.82(2)–93.12(2), 80.85(3)–86.22(3)° respectively).

Although complexes **1H** and **2H** were synthesised previously their solid-state structures were not reported and hence the solid-state structures of **1H–5H** were also determined by single-crystal X-ray diffraction studies and are illustrated in Fig. 6 with pertinent bond lengths compiled in Table 1. In each instance the hydride atom was located in the difference map and was allowed to refine freely. In each complex the Fe^{II} centre adopts a classical piano stool geometry. The Fe–H bond distances in **1H–5H** span the range 1.39(2)–1.60(4) Å. There are only two other examples of terminal iron hydride bonds with bidentate phosphine and cyclopentadienyl ligands with which to compare these values; $[Fe(Cp^*)(H)_2(dppe)][BF_4]$ has $Fe–H_{hydride}$ distances of 1.48 and 1.50 Å[17] and $[Fe(Cp^*)(H)_2(dippe)][BPh_4]$, where dippe = 1,2-bis(diisopropylphosphino)ethane, has $Fe–H_{hydride}$ distances of 1.41(5) and 1.35(6) Å.[18] The Fe–H bond distance in **4H** of 1.39(2) Å, is significantly shorter than those in the rest of the series; however, it is not outside the limited range reported for $Fe–H_{hydride}$ bonds in complexes containing the dppe ligand (1.28(8)–1.65(9) Å).[17,19–35]

Electrochemical investigations

Cyclic voltammetric studies were performed on **1Cl–5Cl**, **1Br–5Br**, **1I–5I** and **1H–5H** as THF solutions containing 0.5 M of electrolyte, $[NBu^n_4][BF_4]$, in the potential range from −2.55 to 1.2 V *vs.* Fc^+/Fc. The results of these studies are summarised in Table 2 and plotted in Fig. 7. THF was chosen as the solvent as it provides good solubility for all of the complexes and remains relatively inert with respect to nucleophilic attack on electrogenerated cations.

The potentials obtained from cyclic voltammetric studies are consistent with results of square wave voltammetry (±0.01 V,

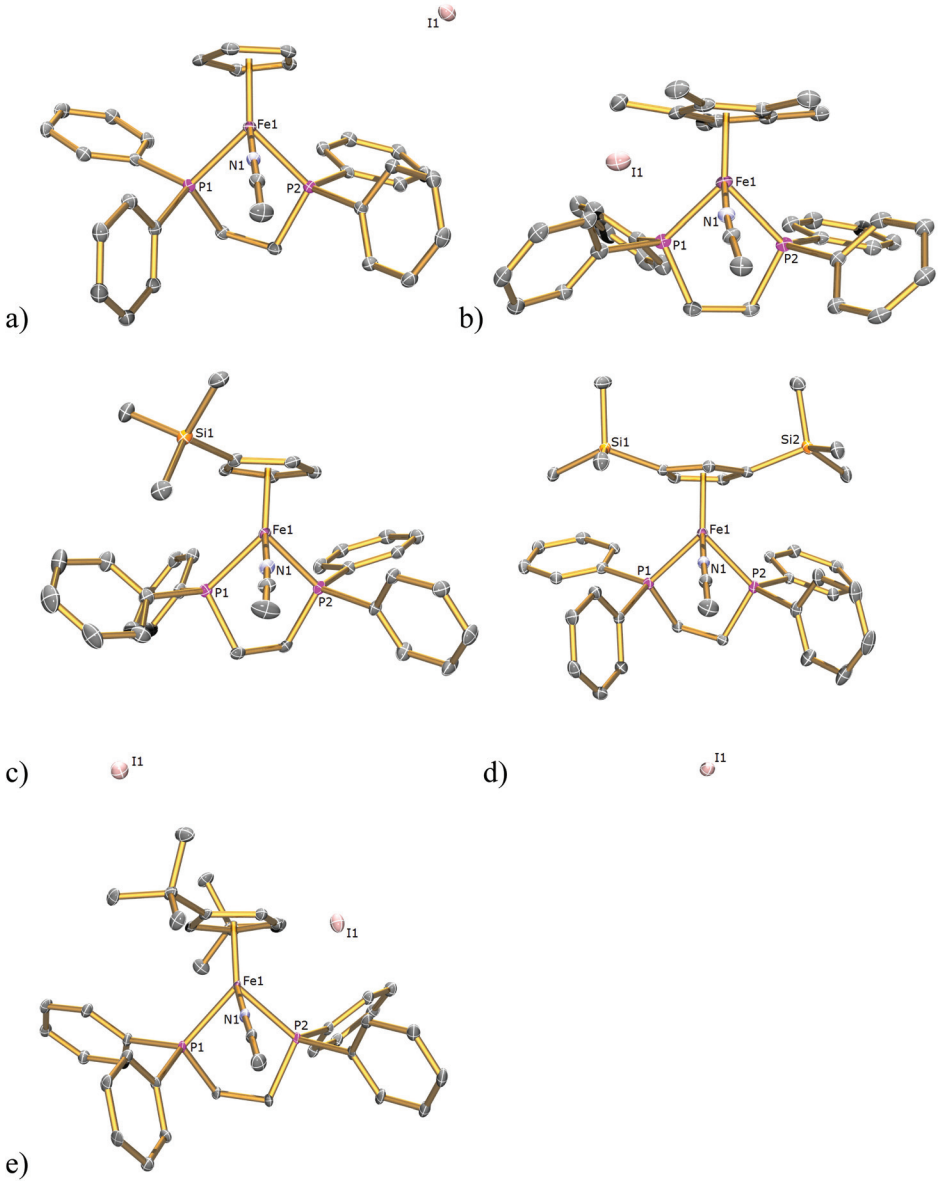

Fig. 5 Solid state structures of (a) **1SIP**, (b) **2SIP**, (c) **3SIP**, (d) **4SIP**, (e) **5SIP** with ellipsoids set at 40% probability. Hydrogen atoms are omitted for clarity.

except **4H**, see below) for the process designated OX and in all cases the potentials are quoted against an appropriate internal standard (see Table S1†). For OX, analysis of the current response in a range of scan rates between 0.02 and 0.3 V s^{-1} suggest that this process is, in general, electrochemically reversible under these conditions, **4H** being an notable exception. At slow scan rates (<0.1 V s^{-1}), the cyclic voltammogram of **4H** has no reduction wave associated with this oxidation suggesting that the electrogenerated cation is unstable. This was confirmed at faster scan rates (1 V s^{-1}), corresponding to shorter timescales, when OX appeared as a redox couple. Data for [Fe(Cp*)(X)(dppe)] (X = Cl, Br, I, and H) have been reported previously wherein this process was assigned as a one electron oxidation to give the corresponding cationic species, [Fe(Cp*)(X)(dppe)].[36] Our results are consistent with these, albeit with a small difference in reported potentials, therefore we assign OX for the series of compounds **1Cl–5Cl**, **1Br–5Br**, **1I–5I** and **1H–5H** as a one-electron oxidation of Fe(II) to Fe(III) corresponding to a $[Fe(Cp^{\dagger})(X)(dppe)]^{+/0}$ couple. The negative values of these potentials, particularly noticeable when referenced against the Fe(III)/Fe(II) couple of ferrocene, are evidence of an electron rich Fe centre, where the loss of an electron is facile. The trend in OX for [Fe($Cp^{\dagger}$)(X)(dppe)] (X = H, Cl, Br and I) always follows H < Cl < Br < I, and it is worthy of note that the difference between OX for $[Fe(Cp^{\dagger})(Cl)(dppe)]^{+/0}$ and $[Fe(Cp^{\dagger})(Br)(dppe)]^{+/0}$ and between $[Fe(Cp^{\dagger})(Br)(dppe)]^{+/0}$ and $[Fe(Cp^{\dagger})(I)(dppe)]^{+/0}$ is +0.04 V and that this difference is independent of the substitutents on the cyclopentadienyl ring.

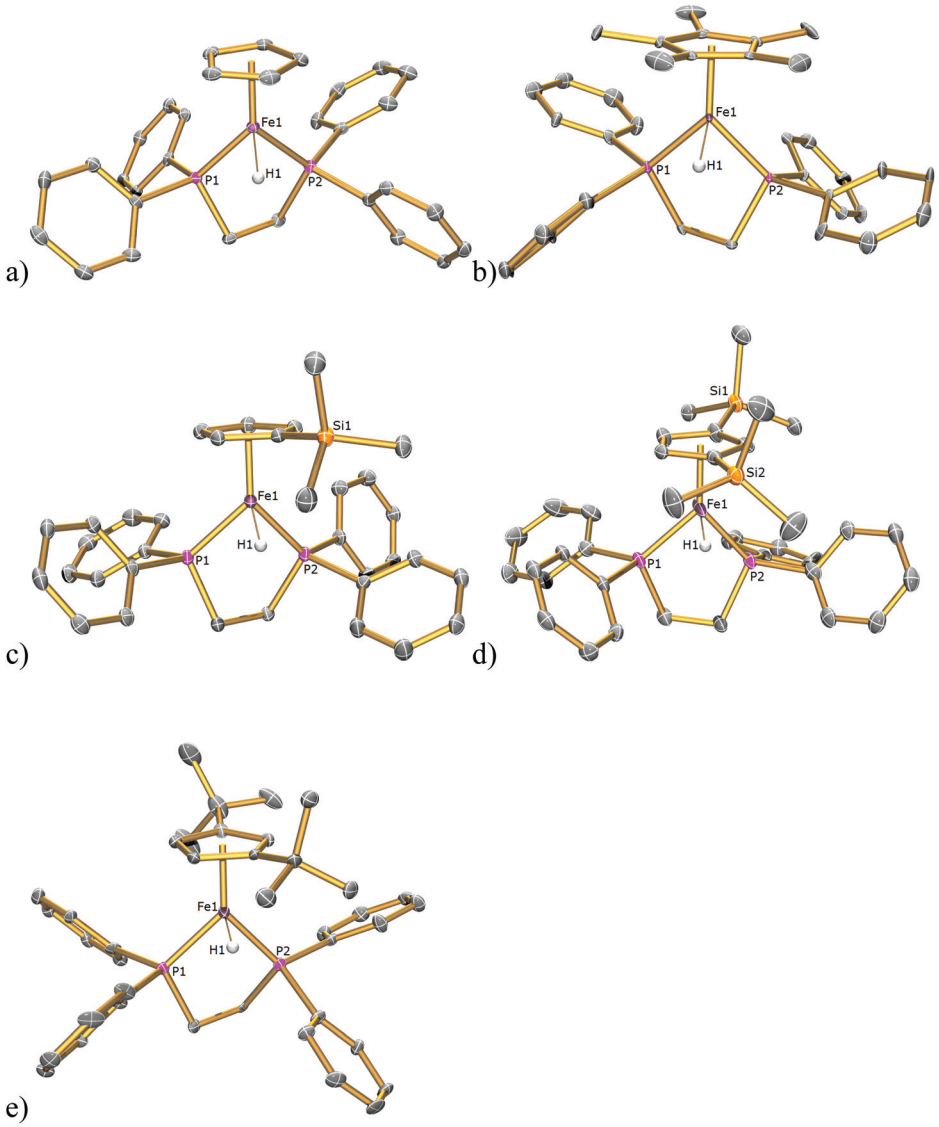

Fig. 6 Solid state structures of (a) **1H**, (b) **2H**, (c) **3H**, (d) **4H**, (e) **5H** with ellipsoids set at 40% probability. All hydrogen atoms except those for the hydride atoms are omitted for clarity.

This trend does not extend to the hydrides, where differences between potentials for $[Fe(Cp^{\dagger})(H)(dppe)]^{+/0}$ and $[Fe(Cp^{\dagger})(Cl)(dppe)]^{+/0}$ vary between +0.05 (Cp′) and +0.12 (Cp*).

The trend in OX for each halide series appears to be inversely correlated with the electronegativity of the halide thus making the chlorides easiest to oxidise and indicating an increase in electron density on the iron centre relative to the corresponding bromides and iodides. This has been rationalised by the involvement of π-based orbitals in the bonding of the halide to the iron centre (see DFT calculations below) thus allowing donation of electron density from the halide to the metal centre. The hydrides should have no contribution from π-bonding so the relatively negative values for OX in $[Fe(Cp^{\dagger})(H)(dppe)]$ compounds reflect the purely σ-bonded nature of the hydrides. The trend in OX for $[Fe(Cp^{\dagger})(Cl)(dppe)]$, $[Fe(Cp^{\dagger})(Br)(dppe)]$ and $[Fe(Cp^{\dagger})(I)(dppe)]$ ($Cp^{\dagger}$ = Cp, Cp*, Cp′, Cp″, Cp^{tt}) follow the series Cp* < Cp^{tt} < Cp′ < Cp″ < Cp and compounds containing Cp* are −0.05 V easier to oxidise than compounds containing Cp^{tt}, Cp^{tt} compounds are −0.09 V easier to oxidise than compounds containing Cp′, Cp′ compounds are −0.01 V easier to oxidise than compounds containing Cp″, and Cp″ compounds are −0.02 V easier to oxidise than compounds containing Cp. Hence compounds containing Cp*, with five electron donating methyl groups are easiest to oxidise whilst compounds containing Cp are most difficult. The latter result is unexpected since TMS is electron withdrawing[37] relative to hydrogen (in Cp) and would be expected to reduce the electron density at iron, thus making oxidation more difficult (hence occurring at a higher potential). However, the difference in OX between [Fe(Cp′)(X)(dppe)] and [Fe(Cp″)(X)(dppe)] (X = Cl, Br and I) is only 0.01 V for the addition of a second TMS group therefore the inductive effect of these substitutents may not be

Table 2 Electrochemical and highest occupied molecular orbital energies for **1Cl–5Cl**, **1Br–5Br**, **1I–5I**, **1H–5H** and **1SIP–5SIP**[a]

Compound	$E_{1/2}$ (V)	HOMO (eV)	Compound	$E_{1/2}$ (V)	HOMO (eV)
1Cl	−0.42	−3.732	**4I**	−0.36	−3.868
2Cl	−0.59	−3.537	**5I**	−0.46	−3.741
3Cl	−0.45	−3.694	**1H**	−0.50	−3.838
4Cl	−0.44	−3.747	**2H**	−0.71	−3.616
5Cl	−0.54	−3.545	**3H**	−0.50	−3.789
1Br	−0.38	−3.788	**4H**	−0.53	−3.706
2Br	−0.55	−3.561	**5H**	−0.62	−3.638
3Br	−0.41	−3.741	**1SIP**	0.26	−7.218
4Br	−0.40	−3.787	**2SIP**	0.06	−6.958
5Br	−0.50	−3.665	**3SIP**	0.25	−7.125
1I	−0.34	−3.836	**4SIP**	0.26	−7.073
2I	−0.51	−3.625	**5SIP**	0.20	−6.997
3I	−0.37	−3.781			

[a] Solutions were *ca.* 0.1 mM of the complex in THF containing 0.5 M $[NBu^n_4][BF_4]$ as the electrolyte for **1Cl–5Cl**, **1Br–5Br**, **1I–5I** and **1H–5H** and *ca.* 0.1 mM of **1I–5I** in MeCN containing 0.1 M $[NBu^n_4][BF_4]$ as the electrolyte for **1SIP–5SIP**. The working electrode was glassy carbon and potentials are reported against the Fc^+/Fc redox couple at ambient temperature. The HOMO energies are derived from the DFT analyses (see below) and are in the gas-phase with no solvent-shell correction.

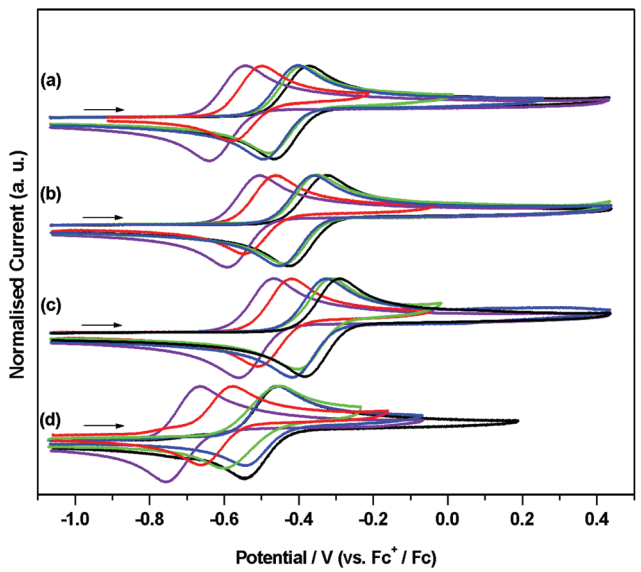

Fig. 7 Cyclic voltammograms showing OX for (a) $[Fe(Cp^\dagger)(Cl)(dppe)]$, (b) $[Fe(Cp^\dagger)(Br)(dppe)]$, (c) $[Fe(Cp^\dagger)(I)(dppe)]$ and (d) $[Fe(Cp^\dagger)(H)(dppe)]$ ($Cp^\dagger$ = Cp (black), Cp* (violet), Cp′ (blue), Cp″ (green), Cp^{tt} (red)). In THF containing $[^nBu_4N][BF_4]$ (0.5 M) as supporting electrolyte, at 0.1 V s^{-1} (except **4H**, at 1 V s^{-1}). Currents are normalised to I_p^a for clarity. Typical currents obtained from CV experiments for $[Fe(Cp^\dagger)(X)(dppe)]$ compounds are shown in Fig. S2† for **1Cl**, as are designations of OX, OX′, OX″ and RED for **1Cl–5Cl**, **1Br–5Br**, **1I–5I** and **1H–5H** used in Table S1.†

transferred effectively to the redox centre, which is reflected by only minor changes in the energies of the HOMO orbitals of the Cp′ and Cp″ derivatives of **1Cl**, **1Br**, and **1I**.

The electrochemistry of the separated ion pairs, $[Fe(Cp^\dagger)(NCMe)(dppe)][I]$ ($Cp^\dagger$ = Cp, Cp*, Cp′, Cp″, Cp^{tt}) was studied by cyclic and square wave voltammetries and the results of these investigations are presented in Table 2 and Fig. S1.† The separated ion pairs were generated *in situ* by dissolving the corresponding $[Fe(Cp^\dagger)(I)(dppe)]$ ($Cp^\dagger$ = Cp, Cp*, Cp′, Cp″, Cp^{tt}) compound in MeCN containing 0.1 M $[NBu^n_4][BF_4]$ as the supporting electrolyte. Analysis of these solutions showed an absence of redox chemistry associated with $[Fe(Cp^\dagger)(I)(dppe)]$ indicating that the equilibrium exclusively favours the formation of the separated ion pair under these conditions. We confirmed the electrochemistry obtained by this method was that associated with a separated ion pair in MeCN solution by dissolving crystals of **2SIP** in MeCN containing 0.1 M $[NBu^n_4][BF_4]$ and repeating the electrochemical experiment; the results of this experiment are essentially identical to those obtained starting from [Fe(Cp*)(I)(dppe)] (Fig. S1†). The displacement of iodide from coordination at the metal centre into the outer sphere significantly complicates the electrochemistry of these compounds since both iodide and $[Fe(Cp^\dagger)(NCMe)(dppe)]^+$ exhibit oxidation chemistry in the range of potentials from *ca.* 0 to +0.5 V. Fig. S1† shows the cyclic voltammetry of the separated ion pairs and $[NBu^n_4][I]$. The electrochemistry of iodide gives two oxidation processes (−0.02 and +0.31 V) and a broad reduction, centred around *ca.* −0.6 V and these may represent electrochemical processes resulting from components of an $[I^-]/[I_2]/[I_3^-]$ equilibrium.[38] The electrochemistry of $[Fe(Cp^\dagger)(NCMe)(dppe)]^+$ ($Cp^\dagger$ = Cp, Cp*, Cp′, Cp″, Cp^{tt}) appears as a redox couple in the range of potentials between +0.06 V (Cp*) and +0.26 V (Cp and Cp″). These potentials are consistent with results of square wave voltammetry (±0.01 V) for the process designated OX (Table S1†). The nature of the electron transfer process in these compounds is difficult to determine given the presence of OX′, a process we assign to iodide oxidation, however it is noted that the separation between E_p^a and E_p^c for OX in $[Fe(Cp^\dagger)(NCMe)(dppe)]^+$ ($Cp^\dagger$ = Cp, Cp*, Cp′, Cp″, Cp^{tt}) compounds (0.09–0.10 V at 0.1 V s^{-1}) is greater than that for the decamethylferrocene couple (0.07 V) used as the internal standard and this suggest that the process is not simply diffusion controlled. For **2SIP**, the electron donating effect of the five methyl groups shift OX to a more negative potential than others in the series and result in OX overlapping with OX′. For the other members of the series OX overlaps with the second oxidation process of the iodide anion. Redox potentials for the separated ion pair complexes are considerably more positive (*ca.* 0.5 V) than those of their $[Fe(Cp^\dagger)(I)(dppe)]$ precursors since oxidation involves the loss of an electron from an already cationic species *i.e.* the $[Fe(Cp^\dagger)(MeCN)(dppe)]^{2+/+}$ redox couple however these potentials are significantly lower than those obtained previously for the 16-electron cationic complex $[Fe(Cp^*)(dppe)][PF_6]$[39] (0.64 V *vs.* Fc^+/Fc in THF) *cf.* 0.06 V for [Fe(Cp*)(NCMe)(dppe)] in MeCN.

Mössbauer studies

The Mössbauer parameters at 80 K for all of the compounds are collected in Table 3. The isomer shift (I.S.) and quadruple splitting (Q.S.) values for all compounds are fully consistent with derivatives of iron(II)–cyclopentadienyl in a

Table 3 Mössbauer data for compounds **1Cl–5Cl**, **1Br–5Br**, **1I–5I**, **1SIP–5SIP** and **1H–5H** at 80 K[a]

Compound	I.S. (mms^{-1})	Q.S. (mms^{-1})	H.W.H.M. (mms^{-1})
1Cl	0.44	1.92	0.13
2Cl	0.48	2.04	0.15
3Cl	0.46	1.88	0.13
4Cl	0.48	1.73	0.13
5Cl	0.50	2.08	0.15
1Br	0.44	1.94	0.13
2Br	0.50	2.10	0.14
3Br	0.47	1.84	0.12
4Br	0.48	1.70	0.13
5Br	0.53	2.00	0.14
1I	0.43	1.89	0.12
2I	0.52	2.09	0.13
3I	0.45	1.85	0.13
4I	0.49	1.69	0.12
5I	0.53	1.95	0.13
1SIP	0.39	2.01	0.14
2SIP	0.42	2.00	0.13
3SIP	0.39	1.91	0.14
4SIP	0.44	1.86	0.14
5SIP	0.45	1.97	0.13
1H	0.26	1.91	0.13
2H	0.25	1.92	0.13
3H	0.26	1.70	0.14
4H	0.28	1.71	0.16
5H	0.27	1.96	0.15

[a] I.S. = isomer shift; Q.S. = quadrupole splitting; H.W.H.M = half-width at half-maxima with errors $\leq \pm 0.01$ mms^{-1}.

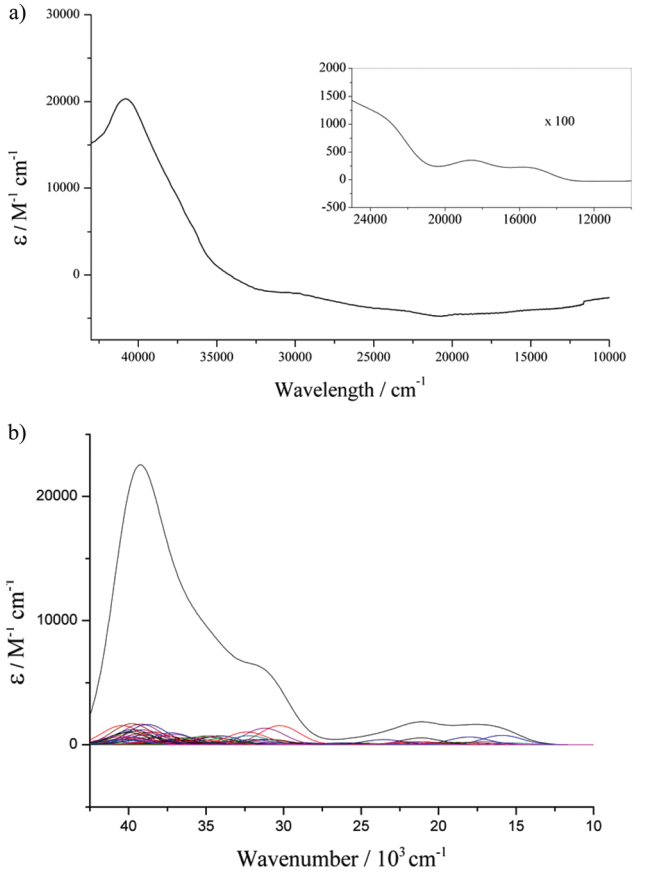

Fig. 8 (a) UV-vis spectra of **2Cl** at 1.25 mM and 0.0125 mM (insert) in THF solution. (b) Predicted UV-vis spectrum of **2Cl** showing the individual electronic transitions and the combined total in the gas phase.

piano-stool geometry.[13,14,40] As expected the I.S. decreases and the Q.S. is invariant on raising the temperature from 80 to 298 K.[41,42] On changing halide from chloride to bromide to iodide and on varying substituents on the cyclopentadienyl ligand there are only slight changes in I.S. and Q.S. When halide is replaced by acetonitrile to form a separated ion pair there is a slight decrease in I.S. but a much larger decrease is observed when halide is replaced by hydride; this can be attributed to the higher σ-donor ability of the hydride ligand increasing the relative electron density at the iron centre.

UV-Vis spectroscopic studies

The UV-vis spectra of all the complexes were recorded in THF solutions at two different concentrations (1.25 mM and 0.0125 mM) to enable observation of all the relevant transitions without interference from solvent overtones. Theoretical UV-vis spectra have also been plotted from time dependant DFT (TD-DFT) calculations. The representative experimental and calculated UV-vis spectra of **2Cl** are illustrated in Fig. 8. At dilute concentration an intense band is observed at 40 816 cm^{-1} (ε = 20 300 M^{-1} cm^{-1}) in the UV region, and at higher concentrations relatively weak bands can be observed in the visible region at 16 502 (ε = 221 M^{-1} cm^{-1}) and 18 587 cm^{-1} (ε = 352 M^{-1} cm^{-1}). By comparison of these experimental data with the combined total of the calculated data it can be seen that they are in good agreement, and that the calculations are a good approximation of the experimental spectra. With this in hand it is then possible to assign these absorptions from the calculated spectra, and calculations suggest that the band at 40 816 cm^{-1}, is a result of π–π* transitions in the aromatic carbon systems; and the bands in the visible region can be predominantly ascribed to metal–ligand charge transfer (MLCT) from the Fe 3d orbitals to the phenyl rings and the Cp* ligand.

The UV-vis spectra for the bromide and iodide series of complexes present similar observations as found in the spectra of the chloride series where variation of the Cp ligands has an effect on the absorptions observed in the visible region (see ESI† for further spectra). However, there is no obvious trend in the electronic absorptions observed upon change in halide across the series, therefore we can conclude that the Fe to Cp MLCT bands are the dominant features in the visible region and the halide has very little effect on the absorptions, Table 4. Although one notable feature is the value of the extinction coefficient for the π–π* transitions in the bromide complexes (**1Br–5Br**) are on average larger than their chloride and iodide counterparts. For example the π–π* transition in **4Br** at 41 152 cm^{-1} has a molar absorptivity of 46 300 M^{-1}

Table 4 Experimental (in THF solution) and calculated (in gas phase) UV-vis absorptions and extinction coefficients for **1Cl–5Cl**, **1Br–5Br**, **1I–5I**, **1SIP–5SIP** and **1H–5H**[a]

Compound	**1Cl**	**2Cl**	**3Cl**	**4Cl**	**5Cl**
Experimental/cm^{-1} (ε/M^{-1} cm^{-1})	17 007 (247)	16 502 (221)	16 978 (376)	15 500 (191)	15 000 (113)
	19 880 (307)	18 587 (352)	19 417 (463)	18 903 (339)	18 148 (183)
	40 323 (21 000)	40 816 (20 300)	41 152 (15 000)	39 682 (13 200)	39 682 (21 900)
Theoretical/cm^{-1}	16 200 (478)	15 900 (1340)	16 400 (1170)	16 600 (1460)	15 400 (412)
	18 400 (1150)	17 600 (1650)	19 100 (1310)	18 400 (1340)	18 500 (1580)
	37 100 (9590)	39 200 (22 600)	35 300 (11 500)	35 600 (11 500)	35 500 (11 300)
Compound	**1Br**	**2Br**	**3Br**	**4Br**	**5Br**
Experimental/cm^{-1} (ε/M^{-1} cm^{-1})	16 155 (200)	15 456 (156)	15 898 (389)	15 898 (334)	15 456 (271)
	19 960 (391)	18 587 (283)	19 417 (617)	18 939 (621)	18 051 (425)
		40 000 (21 900)		41 152 (46 300)	41 152 (30 200)
Theoretical/cm^{-1}		15 300 (577)	16 200 (921)	16 600 (1310)	15 400 (1260)
	18 600 (1030)	18 400 (1320)	19 200 (1390)	18 900 (1450)	18 200 (1810)
	36 900 (8390)	34 800 (11 100)	34 800 (11 100)	34 500 (9930)	34 700 (10 300)
Compound	**1I**	**2I**	**3I**	**4I**	**5I**
Experimental/cm^{-1} (ε/M^{-1} cm^{-1})	16 000 (134)	15 106 (264)	15 848 (199)	15 000 (172)	14 500 (202)
	20 120 (238)	18 519 (500)	19 569 (421)	19 048 (445)	18 051 (448)
	40 323 (19 100)	40 486 (25 000)	40 486 (25 900)	40 486 (19 100)	40 323 (21 000)
Theoretical/cm^{-1}	15 800 (219)	15 400 (441)	15 500 (556)	16 300 (1140)	15 000 (949)
	19 200 (982)	18 200 (1090)	18 800 (1180)	19 100 (1360)	18 500 (1880)
	34 500 (7060)	33 400 (10 300)	34 000 (10 700)	34 300 (10 700)	35 000 (10 900)
Compound	**1SIP**	**2SIP**	**3SIP**	**4SIP**	**5SIP**
Experimental/cm^{-1} (ε/M^{-1} cm^{-1})	16 000 (95)	15 244 (160)		15 015 (123)	14 514 (221)
	20 202 (392)	18 553 (368)	20 921 (658)	19 120 (391)	18 083 (491)
	24 500 (552)	22 750 (809)	40 323 (25 300)	23 000 (458)	22 500 (715)
	40 323 (22 900)	40 323 (32 700)		40 000 (26 700)	40 000 (28 100)
Theoretical/cm^{-1}	21 200 (1180)	19 900 (705)	21 300 (1440)	21 000 (1530)	21 400 (1050)
	25 100 (1170)	25 400 (2030)	26 000 (1530)	27 600 (1800)	26 900 (1830)
	32 700 (10 900)	32 500 (11 900)	32 400 (10 600)	31 900 (10 100)	33 800 (12 100)
	39 600 (12 400)	37 600 (14 900)	38 700 (15 700)	38 100 (12 500)	38 500 (12 200)
Compound	**1H**	**2H**	**3H**	**4H**	**5H**
Experimental/cm^{-1} (ε/M^{-1} cm^{-1})		28 011 (2760)	24 000 (805)	24 096 (1660)	23 474 (2610)
	39 683 (27 900)	39 841 (27 900)	40 161 (8730)	39 683 (14 200)	39 683 (20 500)
Theoretical/cm^{-1}		16 400 (1190)			
	20 600 (3640)	18 600 (2590)	20 200 (3550)	20 300 (3430)	17 900 (2190)
	27 300 (1050)	21 600 (2520)	26 700 (1790)	25 600 (2130)	22 900 (2110)
	37 700 (13 600)	26 400 (1210)	36 700 (12 300)	36 400 (12 600)	27 200 (1620)
		31 300 (5950)			36 000 (15 700)

[a] Epsilon is quoted to 3 significant figures.

cm^{-1} which is at least twice as large as the analogous transition in **4Cl** of ε = 13 200 M^{-1} cm^{-1} at 39 682 cm^{-1}, and **4I** of ε = 19 100 M^{-1} cm^{-1} at 40 486 cm^{-1}.

IR spectroscopic studies

The IR spectra of all the complexes studied in this work were recorded as Nujol mulls. The IR spectra of **1H–2H** contain bands at 1845, 1844, 1849, 1854 and 1872 cm^{-1} respectively and these absorptions can be assigned to the ν_{Fe-H} stretching absorptions for the terminally bonded metal hydride. All these bands are very weak, and are comparable to the ν_{Fe-H} reported for other structurally authenticated iron terminal hydride complexes containing the dppe ligand which span the range 1833–1919 cm^{-1}.[20,30,34] The only other example of an iron hydride complex with both dppe and cyclopentadienyl ligands with which to compare is [Fe(Cp*)(H)(dppe)][PF_6] that has a comparable band at 1869 cm^{-1}.[43]

DFT calculations

We have undertaken DFT calculations for **1Cl–5Cl**, **1Br–5Br**, **1I–5I**, **1SIP–5SIP** and **1H–5H** to provide a qualitative description of the structure and bonding within these complexes and to provide a framework to interpret the electrochemical properties of these compounds. The DFT calculations reproduce the magnitude of the crystallographically determined bond lengths and the interbond angles of these complexes to within ~0.05 Å and ~1.5°, respectively. We therefore conclude that the calculations afford reliable qualitative descriptions of the electronic manifolds of **1Cl–5Cl**, **1Br–5Br**, **1I–5I**, **1SIP–5SIP** and **1H–5H**.

The frontier orbital manifolds of **1Cl–5Cl**, **1Br–5Br** and **1I–5I** are similar with the HOMO, HOMO−1 and HOMO−2 orbitals in each compound possessing dominant Fe character derived from the 3d orbitals that form the t_{2g} set in O_h symmetry (for representative frontier orbitals see Fig. 9).[44] These orbitals are non-bonding with respect to σ-interactions but can

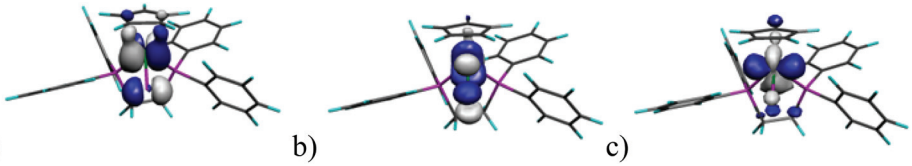

Fig. 9 Frontier Kohn Sham molecular orbitals of **1Cl**: (a) HOMO, (b) HOMO–1, (c) HOMO–2. The models were orientated such that the Fe–X vector corresponded to the *z*-axis and, looking down the Fe–X vector, the left and right Fe-P bonds were aligned along the x and y axes, respectively.

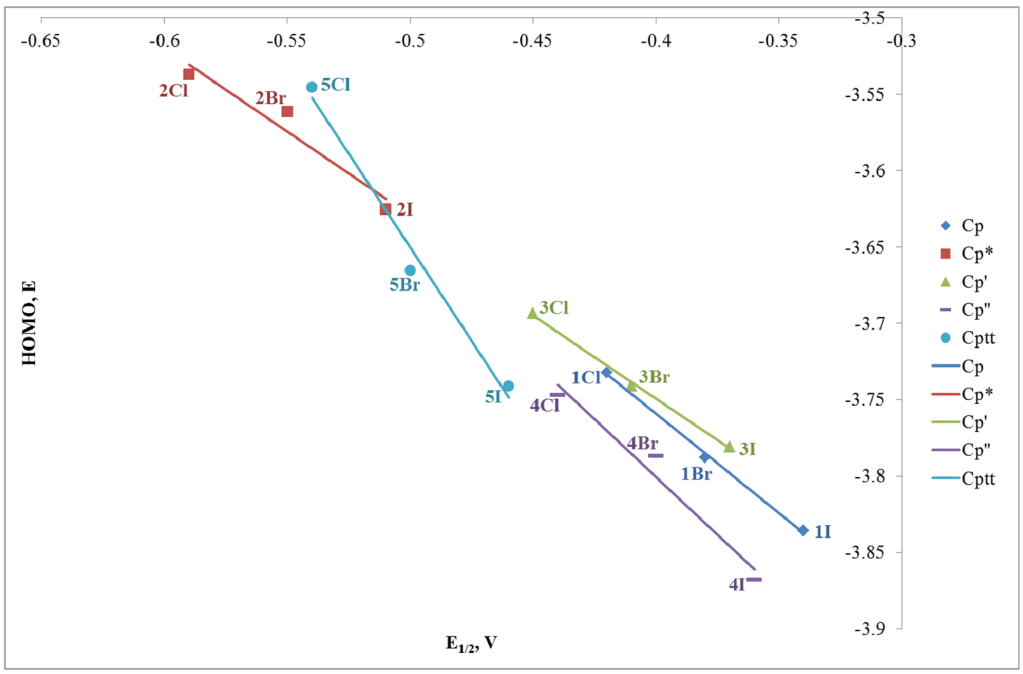

Fig. 10 Plot of HOMO energy *vs.* $E_{\frac{1}{2}}$ for **1Cl–5Cl**, **1Br–5Br** and **1I–5I**.

exhibit π-interactions with X = Cl, Br, I. Thus, in each **1Cl–5Cl**, **1Br–5Br** and **1I–5I** the HOMO possess Fe and X character (61.9–74.0% and 10.7–24.9%, Table S3†) and for a homogeneous series with a fixed cyclopentadienyl-derived ligand the contribution to the HOMO typically varies as I > Br > Cl as would be expected from the π-donor ability for each halogen donor. These calculations are in broad agreement with those accomplished previously for CpFe(dpe)X (dpe = 1,2-diphospinoethane; X = Cl, Br, I).[28] The energies of the HOMO orbital for a fixed Cp ligand and $E_{\frac{1}{2}}$ for the oxidation process (see above) show clear trends as X is varied (Fig. 10). Thus, the energy of the HOMO varies as Cl > Br > I with a reduction potential order of Cl < Br < I. Thus, for a fixed cyclopentadienyl-derived ligand complexes with X = Cl are more readily oxidised to their cationic counterparts and this observation is borne out by the relative energies of the HOMO orbitals in this series of compounds. The variation in energy of the HOMO with X-ligand appears counterintuitive given the percentage X-ligand character in the HOMO and the relative π-donor abilities of the halide donors. This inverse halide order has been noted previously,[39] and has been ascribed to the ionic nature of the Fe–X bond, in which the X-ligand may be viewed as acting as a point negative charge that destabilizes the t_{2g} set of orbitals which results in an inverse of the energy order expected from π-donor effects alone.[45–50]

Conclusions

To conclude, we have reported the synthesis of three iron(II) halide dppe complexes, and their utility in preparing a range of cyclopentadienyl derivatives. In all, we describe the synthesis of twenty five iron cyclopentadienyl dppe complexes as either halide (Cl, Br, I), separated ion pair, or hydride derivatives, thus providing a cohesive and reliable approach to the preparation of such molecules. This report has enabled a comprehensive structural and spectroscopic benchmarking study, providing a detailed understanding of the electronic structure of these compounds in one common framework. The Mössbauer studies suggest that the bonding is these complexes is

predominantly ionic. Nevertheless, it is evident that the cyclopentadienyl and X-ligands modulate the electronic structure and redox properties of iron. Surprisingly, it is clear that although the cyclopentadienyl substituents do influence the redox properties of the iron centre, their influence is modest, and does not follow the trend that might be anticipated. In the pantheon of cyclopentadienyl ligands, taking C_5H_5 as the reference point, the pentamethyl and di-*tert*-butyl variants are usually described as better donor and poorer acceptor ligands, whereas the silyl-substituted variants are often viewed as poorer donors and better acceptor ligands. This should result in pentamethyl and di-*tert*-butyl cyclopentadienyl ligands leading to more electron rich iron centres whereas the silyl-substituted variants should give more electron deficient iron centres. However, on the basis of the electrochemical data presented here although the alkyl-cyclopentadienyls do fit this trend, this view is clearly overly simplistic where the silyl-substituted variants are concerned since their behaviour more closely resembles that of C_5H_5. This observation helps to codify the unpredictability of cyclopentadienyl-substituent effects on the redox potentials of transition metal complexes for a widely employed ligand class. The identity of the X-ligand, however, has a substantial and direct effect on the redox properties of the iron centre, which reflects the potential π-donor capcacity of the halides and their direct negative point charge to iron; indeed for the halides there is an essentially linear electrochemical relationship on moving from Cl to Br to I and these studies support the notion of hydride as a strong donor ligand. The complexes reported in this study could find extensive utility in molecular wire and metal–metal bond chemistry, where control of redox properties is important; the data presented here provide a database that enables the selection of a particular iron complex with an appropriate reduction potential for a given application. We are currently investigating the utility of the iron-hydride complexes presented here for the synthesis of uranium–iron bonds by alkane or amine elimination routes.

Experimental

General experimental details

All manipulations were carried out using standard Schlenk techniques or an MBraun UniLab glovebox, under an atmosphere of dry nitrogen. THF, toluene, hexane and diethyl ether were dried by passage through activated alumina towers and degassed before use and then were stored over potassium mirrors (except THF which was stored over activated 4 Å molecular sieves). Acetonitrile and dichloromethane were distilled from CaH_2 and stored over 3 Å (DCM) or 4 Å (MeCN) activated molecular sieves. Benzene-d_6 was dried over potassium, distilled, degassed and stored under nitrogen. The compounds CpH*,[51,52] KCp*,[53] $C_5H_5(SiMe_3)$,[54] $KC_5H_4(SiMe_3)$,[54] $C_5H_4(SiMe_3)_2$,[54] $KC_5H_3(SiMe_3)_2$,[54] $C_5H_4(^tBu)_2$,[55] $KC_5H_3(^tBu)_2$,[55] and $[FeCl_2(dppe)]$[55] were synthesised according to published procedures. The compounds LiCp, NaCp and KCp were purchased from Sigma Aldrich and were used without any further purification. Compounds **II**, **III**, **2Cl**, **1I**, and **1H** have previously been reported and are well characterised, the syntheses described for these compounds below are for completeness and to report any additional characterisation.

NMR spectra were recorded on either a Bruker DPX300 spectrometer [operating at 300.1 MHz (^{1}H), 75.5 MHz ($^{13}C\{^1H\}$) and 121.5 MHz ($^{31}P\{^1H\}$)] or a Bruker DPX400, AV400 spectrometer [operating at 400.2 MHz (^{1}H), 100.6 MHz ($\{^{13}C\{^1H\}$), 162.0 MHz ($^{31}P\{^1H\}$) and 79.5 MHz ($^{29}Si\{1H\}$)]. Chemical shifts are quoted in ppm and are relative to TMS (^{1}H, $^{13}C\{^1H\}$ and $^{29}Si\{^1H\}$) and external 85% H_3PO_4 ($^{31}P\{^1H\}$). IR spectra were recorded on a Bruker Tensor 27 FTIR spectrometer, where samples were prepared in the glovebox using a Nujol mull between two KBr discs. UV-Vis/NIR spectra were recorded on a Perkin Elmer LAMBDA 750 spectrometer. Data were collected in THF in 1 cm path length quartz cuvettes which were prepared in the glovebox. Elemental microanalyses were carried out by Mr Stephen Boyer at the Microanalysis Service, London Metropolitan University, UK or Dr Tong Liu, University of Nottingham. Mössbauer spectra were recorded in a zero magnetic field at 80 K or 298 K on an ES-Technology MS-105 Mössbauer spectrometer with a 25 MBq ^{57}Co source in a rhodium matrix at ambient temperature. Spectra were referenced against a 25 μm iron foil at 298 K and spectrum parameters were obtained by fitting with Lorentzian lines. Samples were prepared by grinding with boron nitride before mounting.

Preparation of $[FeBr_2(dppe)]$, II

THF (40 mL) was added to a mixture of $FeBr_2$ (3.45 g, 16.0 mmol) and dppe (6.43 g, 16.0 mmol) at room temperature and then refluxed overnight. The mixture was filtered, the solids washed with toluene and dried *in vacuo* to yield a light green solid in excellent yield (9.28 g, 94%).

Preparation of $[FeI_2(dppe)]$, III

THF (40 ml) was added to a mixture of FeI_2 (5.00 g, 16.0 mmol) and dppe (6.43 g, 16.0 mmol) at room temperature and stirred for 18 hours. The mixture was filtered and the solids were dried *in vacuo* to yield a yellow solid in excellent yield (10.8 g, 95%).

General preparative method for 1Cl–5Cl, 1Br–5Br, 1I–5I

Toluene (20 ml) was added dropwise to a mixture of FeX_2(dppe) (where X = Cl, Br or I) and MCp† (where M = Li, K or Na, Cp = C_5H_5, M = K, Cp = C_5Me_5, $C_5H_4(SiMe_3)$, $C_5H_3(SiMe_3)_2$ or $C_5H_3(^tBu)_2$) in a 1 : 1 molar ratio at −78 °C with stirring, the resultant mixture was allowed to warm to room temperature slowly over 18 hours. The mixture was filtered and the solids washed with toluene (2 × 5 ml), the volatiles were removed *in vacuo* and the resulting solids were recrystallized from the minimum amount of toluene with storage at −30 °C, with the exception of **1Cl** which is best recrystallized from a DCM/hexane layer (1 : 3 ratio) with storage at −30 °C. The black crystals were isolated by filtration, washed with hexanes (2 × 1–2 mL) and dried *in vacuo*.

1Cl: I (2.63 g, 5.0 mmol) and LiCp (0.36 g, 5.0 mmol), yield: 1.75 g, 66%. Anal. calc'd for $C_{31}H_{29}FeClP_2$: C, 67.11; H, 5.27%. Found: C, 66.85; H, 5.16%. ^{1}H NMR (C_6D_6, 298 K): δ_H 2.29 (m, 4H, CH_2), 4.28 (s, 5H, C_5H_5), 7.01–8.23 (m, 20H, Ar–*H*). ^{13}C{^{1}H} NMR (C_6D_6, 298 K): δ_C 27.65 (t, *C*H$_2$, $^1J_{CP}$ = 81 Hz), 76.94 (C_5H_5), 127.88 (Ar–*C*), 128.22 (Ar–*C*), 128.90 (Ar–*C*), 129.60 (Ar–*C*), 132.31 (t, Ar–*C*, $^2J_{CP}$ = 18 Hz), 134.62 (t, Ar–*C*, $^2J_{CP}$ = 18 Hz), 142.31 (Ar–*C*), 142.67 (Ar–*C*). ^{31}P{^{1}H} NMR (C_6D_6, 298 K): δ_P 111.31. FTIR ν/cm^{-1} (Nujol): 1403 (s), 861 (s), 694 (s), 667 (s) 651 (s), 588 (s), 529 (s) 518 (s), 491 (s), 462 (s) and 438 (s). UV-vis (THF): λ_{max}/cm^{-1} (ε/mol^{-1} cm^{-1}) 17 007 (247), 19 881 (307), 40 323 (21 000). Mössbauer (80 K, mm s^{-1}) I.S. = 0.44, Q.S. = 1.92. CV (298 K, THF, [NBu$_4^n$][[BF$_4$], 1 mM) $E_{1/2}$ = −0.42 V.

2Cl: I (2.63 g, 5.0 mmol) and KCp* (0.87, 5.0 mmol), yield: 2.28 g, 73%. ^{1}H NMR (C_6D_6, 298 K): δ_H 1.40 (s, 15H, CH_3), 2.75 (m, 4H, CH_2), 7.00–8.05 (m, 20H, Ar–*H*). ^{13}C{^{1}H} NMR (C_6D_6, 298 K): δ_C 30.2 (*C*H$_2$), 83.60 (C_5H_5), 131.3–140.2 (Ar–*C*). ^{31}P{^{1}H} NMR (C_6D_6, 298 K): δ_P 91.6. FTIR ν/cm^{-1} (Nujol): 1483(w), 1432 (s), 1091 (s), 1068 (w), 1027 (m), 787 (w), 471 (s), 694 (vs), 658 (s), 616 (w), 528 (vs), 519 (w), 484 (vs), 450 (w) and 428 (s). UV-vis (THF): λ_{max}/cm^{-1} (ε/mol^{-1} cm^{-1}) 16 502 (221), 18 587 (352), 40 816 (20 300). Mössbauer (80 K, mm s^{-1}) I.S. = 0.48, Q.S. = 2.04. CV (298 K, THF, [NBu$_4^n$][[BF$_4$], 1 mM) $E_{1/2}$ = −0.59 V.

3Cl: I (1.05 g, 2.0 mmol) and $KC_5H_4(SiMe_3)$ (0.35 g, 2.0 mmol), yield: 0.66 g, 48%. Anal. calc'd for $C_{33}H_{37}FeClP_2Si$: C, 65.13; H, 5.95%. Found: C, 64.85; H, 6.12%. ^{1}H NMR ($CDCl_3$, 298 K): δ_H 0.08 (s, 9H, CH_3), 2.39 (m, 4H, CH_2), 4.09 (t, 2H, C*H*), 4.31 (t, 2H, C*H*), 7.27–8.14 (m, 20H, Ar–*H*). ^{13}C{^{1}H} NMR ($CDCl_3$, 298 K): δ_C 1.03 (Si*C*H$_3$), 27.20 (*C*H$_2$), 68.95 (*C*H), 77.25 (*C*SiMe$_3$), 88.78 (*C*H), 127.86 (Ar–*C*), 127.97 (Ar–*C*), 129.12 (Ar–*C*), 129.41 (Ar–*C*), 132.29 (Ar–*C*), 134.24 (Ar–*C*). ^{31}P-{^{1}H} NMR ($CDCl_3$, 298 K): δ_P 93.9. ^{29}Si{^{1}H} ($CDCl_3$, 298 K): δ_{Si} −21.94. FTIR ν/cm^{-1} (Nujol): 1658 (s), 1433 (s), 1304 (m), 1245 (s), 1180 (s), 1158 (s), 1070 (s), 1041 (s), 900 (s), 871 (s), 817 (s), 737 (s), 697 (s) 669 (s), 645 (s), 635 (s), 609 (s), 530 (s), 520 (s), 489 (s), 452 (s), 436 (s) and 424 (s). UV-vis (THF): λ_{max}/cm^{-1} (ε/mol^{-1} cm^{-1}) 16 978 (376), 19 417 (463), 41 152 (15 000). Mössbauer (80 K, mm s^{-1}) I.S. = 0.46, Q.S. = 1.88. CV (298 K, THF, [NBu$_4^n$][[BF$_4$], 1 mM) $E_{1/2}$ = −0.45 V.

4Cl: I (0.53 g, 1.0 mmol) and $KC_5H_3(SiMe_3)_2$ (0.25 g, 1.0 mmol), yield: 0.36 g, 51%. Anal. calc'd for $C_{37}H_{45}FeClP_2Si_2$: C, 63.56; H, 6.49%. Found: C, 60.26; H, 6.61%. ^{1}H NMR ($CDCl_3$, 298 K): δ_H 0.25 (s, 18H, CH_3), 2.75 (m, 4H, CH_2), 4.31 (d, 2H, C*H*), 4.85 (s, 1H, C*H*), 7.25–7.94 (m, 20H, Ar–*H*). ^{13}C{^{1}H} NMR (C_6D_6, 298 K): δ_C 0.04 (*C*H$_3$), 28.95 (t, *C*H$_2$, $^1J_{CP}$ = 36 Hz), 77.04 (*C*H), 81.43 (*C*SiMe$_3$), 102.97 (*C*H), 127.74 (Ar–*C*), 129.29 (Ar–*C*), 133.38 (Ar–*C*), 134.33 (Ar–*C*), 140.13 (Ar–*C*). ^{31}P-{^{1}H} NMR (C_6D_6, 298 K): δ_P 93.6. ^{29}Si{^{1}H} ($CDCl_3$, 298 K): δ_{Si} −2.79. FTIR ν/cm^{-1} (Nujol): 1434 (s), 1401 (s), 1251 (s), 1188 (s), 1156 (s), 916 (s), 883 (s), 834 (s), 762 (s), 751 (s), 738 (s), 696 (s), 661 (s), 632 (s), 616 (s), 598 (s), 530 (s), 518 (s), 485 (s), 459 (s), 443 (s) and 426 (s). UV-vis (THF): λ_{max}/cm^{-1} (ε/mol^{-1} cm^{-1}) 15 500 (191), 18 904 (339), 39 683 (13 200). Mössbauer (80 K, mm s^{-1}) I.S. = 0.48, Q.S. = 1.73. CV (298 K, THF, [NBu$_4^n$][[BF$_4$], 1 mM) $E_{1/2}$ = −0.44 V.

5Cl: I (1.05 g, 2.0 mmol) and $KC_5H_3(^tBu)_2$ (0.43 g, 2.0 mmol), yield: 0.76 g, 57%. Anal. calc'd for $C_{39}H_{45}FeClP_2$: C, 70.23; H, 6.80%. Found: C, 70.39; H, 6.72%. ^{1}H NMR ($CDCl_3$, 298 K): δ_H 0.94 (s, 18H, CH_3), 2.26 (s, 4H, CH_2), 3.14 (s, 2H, C=C*H*), 3.99 (d, 1H, C=C*H*), 7.30–7.68 (m, 20H, Ar–*H*). ^{13}C{^{1}H} NMR (C_6D_6, 298 K): δ_C 1.18 (*C*H$_3$), 31.25 (*C*H$_2$), 61.21 (*C*H), 63.14 (*C*H), 76.27 (*C*^{t}Bu), 109.55 (*C*Me$_3$), 126.12 (Ar–*C*), 129.00 (Ar–*C*), 130.15 (Ar–*C*), 134.34 (Ar–*C*), 139.80 (Ar–*C*). ^{31}P{^{1}H} NMR ($CDCl_3$, 298 K): δ_P 85.6. FTIR ν/cm^{-1} (Nujol): 1433 (s), 1183 (s), 1160 (s), 937 (s), 919 (s), 875 (s), 833 (s), 748 (s), 694 (s), 671 (s), 648 (s), 636 (s), 616 (s), 528 (s), 517 (s), 508 (s), 489 (s), 475 (s) and 438 (s). UV-vis (THF): λ_{max}/cm^{-1} (ε/mol^{-1} cm^{-1}) 15 000 (114), 18 149 (183), 39 683 (21 900). Mössbauer (80 K, mm s^{-1}) I.S. = 0.50, Q.S. = 2.08. CV (298 K, THF, [NBu$_4^n$]-[[BF$_4$], 1 mM) $E_{1/2}$ = −0.54 V.

1Br: II (1.23 g, 2.0 mmol) and KCp (0.21 g, 2.0 mmol), yield: 0.52 g, 68%. Anal. Calc'd for $C_{31}H_{29}P_2FeBr$: C, 62.13; H, 4.88%. Found: C, 62.25; H, 5.03%. ^{1}H NMR (C_6D_6, 298 K): δ_H 2.40 (m, 4H, CH_2,), 4.28 (s, 5H, C*H*), 7.01–8.23 (m, 20H, C*H*). ^{13}C{^{1}H} NMR (C_6D_6, 298 K): δ_C 76.64 (*C*H), 128.57 (Ar–*C*), 129.37 (Ar–*C*), 131.97 (Ar–*C*), 134.43 (Ar–*C*). ^{31}P{^{1}H} NMR (C_6D_6, 298 K): δ_P 98.2. FTIR ν/cm^{-1} (Nujol): 1433 (s), 1179 (s), 1156 (s), 861 (s), 846 (s), 831 (s), 812 (s), 787 (s), 743 (s), 727 (s), 694 (s), 669 (s), 652 (s), 588 (s), 528 (s), 518 (s), 489 (s) and 461 (s). UV-vis (THF): λ_{max}/cm^{-1} (ε/mol^{-1} cm^{-1}) 16 155 (200), 19 960 (392). Mössbauer (80 K, mm s^{-1}) I.S. = 0.44, Q.S. = 1.94. CV (298 K, THF, [NBu$_4^n$][[BF$_4$], 1 mM) $E_{1/2}$ = −0.38 V.

2Br: II (1.23 g, 2.00 mmol) and KCp* (0.35 g, 2.00 mmol), yield: 0.40 g, 30%. Anal. Calc'd for $C_{36}H_{39}P_2FeBr$: C, 64.60; H, 5.87%. Found: C, 64.52; H, 6.02%. ^{1}H NMR (C_6D_6, 298 K): δ_H 1.58 (s, 15H, CH_3), 2.35 (m, 4H, CH_2), 7.11–7.40 (m, 20H, Ar–*H*). ^{13}C{^{1}H} NMR (C_6D_6, 298 K): δ_C 11.24 (*C*H$_3$), 31.90 (*C*H$_2$), 83.30 (*C*H), 127.09 (Ar–*C*), 127.18 (Ar–*C*), 128.68 (Ar–*C*), 129.08 (Ar–*C*), 134.45 (t, Ar–*C*, $^2J_{CP}$ = 20 Hz), 135.00 (t, Ar–*C*, $^2J_{CP}$ = 16 Hz), 140.20 (Ar–*C*), 140.50 (Ar–*C*). ^{31}P{^{1}H} NMR (C_6D_6, 298 K): δ_P 95.0. FTIR ν/cm^{-1} (Nujol): 1432 (s), 1179 (s), 1153 (s), 1067 (s), 865 (s), 740 (s), 699 (s), 662 (s), 617 (s), 528 (s), 490 (s), 468 (s) and 433 (s). UV-vis (THF): λ_{max}/cm^{-1} (ε/mol^{-1} cm^{-1}) 15 455 (157), 18 587 (284), 40 000 (21 900). Mössbauer (80 K, mm s^{-1}) I.S. = 0.52, Q.S. = 2.09. CV (298 K, THF, [NBu$_4^n$][[BF$_4$], 1 mM) $E_{1/2}$ = −0.55 V.

3Br: II (1.23 g, mmol) and $KC_5H_4(SiMe_3)$ (0.35 g, 2.0 mmol), yield: 0.52 g, 39%. Anal. Calc'd for $C_{34}H_{36}P_2SiFeBr$: C, 60.82; H, 5.55%. Found: C, 61.95; H, 5.40%. ^{1}H NMR (C_6D_6, 298 K): δ_H 0.39 (9H, s, CH_3), 2.41 (m, 4H, CH_2), 3.29 (d, 2H, C*H*), 5.15 (d, 2H, C*H*), 7.02–8.18 (m, 20H, Ar–*H*). ^{13}C{^{1}H} NMR (C_6D_6, 298 K): δ_C 0.15 (*C*H$_3$), 27.93 (t, *C*H$_2$, $^1J_{CP}$ = 76 Hz), 70.42 (*C*H), 86.86 (*C*H), 128.68 (Ar–*C*), 129.34 (Ar–*C*), 132.39 (Ar–*C*), 134.51 (Ar–*C*). ^{31}P{^{1}H} NMR (C_6D_6, 298 K): δ_P 95.9. ^{29}Si{^{1}H} NMR (C_6D_6, 298 K): δ_{Si} −2.3. FTIR ν/cm^{-1} (Nujol): 1245 (s), 1180 (s), 1154 (s), 914 (s), 885 (s), 831 (s), 740 (s), 659 (s), 655 (s), 635 (s), 532 (s), 517 (s), 482 (s) and 455 (s). UV-vis (THF): λ_{max}/cm^{-1} (ε/mol^{-1} cm^{-1}) 15 898 (390), 19 417 (618). Mössbauer (80 K, mm s^{-1}) I.S. = 0.47, Q.S. = 1.84. CV (298 K, THF, [NBu$_4^n$][[BF$_4$], 1 mM) $E_{1/2}$ = −0.41 V.

4Br: II (1.23 g, 2.0 mmol) and $KC_5H_3(SiMe_3)_2$ (0.50 g, 2.0 mmol), yield: 0.69 g, 46%. Anal. Calc'd for $C_{37}H_{45}P_2Si_2FeBr$: C, 59.76; H, 6.10%. Found: C, 59.85; H, 5.91%. ^{1}H NMR (C_6D_6, 298 K): δ_H 0.22 (s, 18H, CH_3), 2.35 (m, 4H, CH_2), 4.02 (s, 2H, C*H*), 5.43 (s, 1H, C*H*), 7.08–7.40 (m, 20H, Ar–*H*). ^{13}C{^{1}H} NMR (C_6D_6, 298 K): δ_C 0.41 (*C*H_3), 29.45 (*C*H_2), 78.61 (*C*H), 81.12 (*C*H), 101.60 (Ar–*C*), 127.56–134.67 (Ar–*C*). ^{31}P{^{1}H} NMR (C_6D_6, 298 K): δ_P 90.2. ^{29}Si{^{1}H} NMR (C_6D_6, 298 K): δ_{Si} −2.6. FTIR ν/cm^{-1} (Nujol): 1432 (s), 1366 (s), 1331 (s), 12 580 (s), 1238 (s), 1187 (s), 1161 (s), 1068 (s), 1051 (s), 968 (s), 956 (s), 923 (s), 887 (s), 833 (s), 751 (s), 733 (s), 692 (s), 656 (s), 629 (s), 611 (s), 585 (s), 532 (s), 519 (s), 483 (s), 448 (s), 438 (s) and 425 (s). UV-vis (THF): λ_{max}/cm^{-1} (ε/mol^{-1} cm^{-1}) 15 898 (334), 18 939 (622), 41 152 (46 300). Mössbauer (80 K, mm s^{-1}) I.S. = 0.49, Q.S. = 1.69. CV (298 K, THF, [NBu$_4^n$][[BF$_4$], 1 mM) $E_{1/2}$ = −0.40 V.

5Br: II (1.23 g, 2.0 mmol) and $KC_5H_3(^tBu)_2$ (0.42 g, 2.0 mmol), yield: 0.79 g, 56%. Anal. Calc'd for $C_{39}H_{45}P_2FeBr$: C, 65.82; H, 6.38%. Found: C, 65.67; H, 6.36%. ^{1}H NMR (C_6D_6, 298 K): δ_H 1.26 (s, 18H, CH_3), 2.23 (m, 4H, CH_2), 3.39 (s, 2H, C*H*), 5.29 (s, 1H, C*H*), 7.12–7.27 (m, 20H, Ar–*H*). ^{13}C{^{1}H} NMR (C_6D_6, 298 K): δ_C 1.17 (*C*H_3), 31.54 (t, *C*H_2, $^1J_{CP}$ = 278 Hz), 60.93 (*C*H), 80.63 (*C*H), 107.06 (Ar–*C*), 127.88 (Ar–*C*), 129.01 (Ar–*C*), 134.26 (Ar–*C*). ^{31}P{^{1}H} NMR (C_6D_6, 298 K): δ_P 82.7. FTIR ν/cm^{-1} (Nujol): 1659 (s), 1433 (s), 1286 (s), 1251 (s), 1187 (s), 1160 (s), 1047 (s), 998 (s), 934 (s), 919 (s), 872 (s), 843 (s), 832 (s), 791 (s), 741 (s), 691 (s), 664 (s), 655 (s), 642 (s), 615 (s), 528 (s), 482 (s), 450 (s) and 428 (s). UV-vis (THF): λ_{max}/cm^{-1} (ε/mol^{-1} cm^{-1}) 15 456 (271), 18 051 (425), 41 152 (30 200). Mössbauer (80 K, mm s^{-1}) I.S. = 0.53, Q.S. = 1.95. CV (298 K, THF, [NBu$_4^n$][[BF$_4$], 1 mM) $E_{1/2}$ = −0.50 V.

1I: III (1.42 g, 2.0 mmol) and NaCp (0.16 g, 2.0 mmol), yield: 0.84 g, 67%. ^{1}H NMR (C_6D_6, 298 K): δ_H 2.60 (m, 4H, CH_2), 4.30 (s, 5H, C_5H_5), 6.99–8.05 (m, 20H, Ar–*H*); ^{31}P{^{1}H} NMR (C_6D_6, 298 K): δ_P 99.1. UV-vis (THF): λ_{max}/cm^{-1} (ε/mol^{-1} cm^{-1}) 16 000 (69.2), 20 120 (219), 40 323 (19 300). Mössbauer (80 K, mm s^{-1}) I.S. = 0.43, Q.S. = 1.89. CV (298 K, THF, [NBu$_4^n$][[BF$_4$], 1 mM) $E_{1/2}$ = −0.34 V.

2I: III (0.71 g, 1.0 mmol) and KCp* (0.17 g, 1.0 mmol), yield: 0.46 g, 64%. Anal. calc'd for $C_{36}H_{39}FeIP_2$: C, 60.36; H, 5.49%. Found: C, 60.26; H, 5.37%. ^{1}H NMR (C_6D_6, 298 K): δ_H 1.17 (s, 15H, CH_3), 2.50 (m, 4H, CH_2), 6.82–8.14 (m, 20H, Ar–*H*); ^{13}C{^{1}H} NMR (C_6D_6, 298 K): δ_C −11.24 (*C*H_3), 31.90 (t, *C*H_2) 83.30 (H*C*═C) 128.81 (*p*-Ar–*C*), 129.48 (*m*-Ar–*C*), 133.14 (*o*-Ar–*C*), 134.73 (*i*-Ar–C); ^{31}P{^{1}H} NMR (C_6D_6, 298 K): δ_P 95.0. FTIR ν/cm^{-1} (Nujol): 1179 (s), 1153 (s), 1069 (s), 893 (s), 863 (s), 739 (s), 699 (s), 660 (s), 618 (s), 527 (s), 518 (s), 490 (s), 468 (s), 451 (s) and 431 (s). UV-vis (THF): λ_{max}/cm^{-1} (ε/mol^{-1} cm^{-1}) 15 106 (264), 18 518 (500), 40 486 (35 000). Mössbauer (80 K, mm s^{-1}) I.S. = 0.52, Q.S. = 2.09. CV (298 K, THF, [NBu$_4^n$][[BF$_4$], 1 mM) $E_{1/2}$ = −0.51 V.

3I: III (0.71 g, 1.0 mmol) and $KC_5H_4(SiMe_3)$ (0.18 g, 1.0 mmol), yield: 0.26 g, 36%. Anal. calc'd for $C_{34}H_{37}FeIP_2Si$: C, 56.84; H, 5.19%. Found: C, 57.50; H, 5.18%. ^{1}H NMR (C_6D_6, 298 K): δ_H 0.38 (s, 9H, CH_3), 2.57 (m, 4H, CH_2), 3.45 (s, 2H, C*H*), 5.14 (s, 2H, C*H*), 6.99–8.14 (m, 20H, Ar–*H*). ^{13}C{^{1}H} NMR (C_6D_6, 298 K): δ_C 0.59 (Si*C*H_3), 28.78 (t, *C*H_2, $^1J_{CP}$ = 84 Hz), 71.71 (*C*H), 81.94 (t, *C*SiMe$_3$, $^2J_{CP}$ = 8 Hz), 86.50 (*C*H), 127.63 (Ar–*C*), 127.73 (Ar–*C*), 128.58 (Ar–*C*), 129.32 (Ar–*C*), 132.35 (t, Ar–*C*, $^2J_{CP}$ = 16 Hz), 132.90 (t, Ar–*C*, $^2J_{CP}$ = 32 Hz) 134.48 (t, Ar–*C*, $^2J_{CP}$ = 16 Hz), 139.33 (t, Ar–*C*, $^2J_{CP}$ = 24 Hz), 139.74 (t, Ar–*C*, $^2J_{CP}$ = 20 Hz) 142.00 (t, Ar–*C*, $^1J_{CP}$ = 52 Hz), 142.33 (t, Ar–*C*, $^1J_{CP}$ = 52 Hz). ^{31}P{^{1}H} NMR (C_6D_6, 298 K): δ_P 96.8. ^{29}Si{^{1}H} (C_6D_6, 298 K): δ_{Si} −1.79. FTIR ν/cm^{-1} (Nujol): 1482 (w), 1431 (s), 1308 (w), 1243 (m), 1156 (m), 1096 (m), 1069 (sh), 1037 (sh), 1026 (w), 999 (w), 900 (w), 890 (w), 833 (s), 741 (s), 693 (vs), 661 (s), 632 (m), 617 (sh), 566 (w), 518 (vs), 485 (s) and 436 (s). UV-vis (THF): λ_{max}/cm^{-1} (ε/mol^{-1} cm^{-1}) 15 848 (199), 19 569 (421), 40 486 (25 900). Mössbauer (80 K, mm s^{-1}) I.S. = 0.45, Q.S. = 1.85. CV (298 K, THF, [NBu$_4^n$][[BF$_4$], 1 mM) $E_{1/2}$ = −0.37 V.

4I: III (0.71 g, 1.0 mmol) and $KC_5H_3(SiMe_3)_2$ (0.25 g, 1.0 mmol), yield: 0.41 g, 52%. Anal. calc'd for $C_{37}H_{45}FeIP_2Si_2$: C, 56.21; H, 5.74%. Found: C, 56.30; H, 5.65%. ^{1}H NMR (C_6D_6, 298 K): δ_H 0.24 (s, 18H, CH_3), 2.50 (m, 4H, CH_2), 4.04 (s, 2H, C*H*), 5.56 (s, H, C*H*), 6.95–8.28 (m, 20H, Ar–*H*). ^{13}C{^{1}H} NMR (C_6D_6, 298 K): δ_C 0.70 (Si*C*H_3), 30.46 (*C*H_2), 79.00 (*C*H), 79.61 (*C*H), 101.70 (*C*SiMe$_3$) 127.70 (Ar–*C*), 127.94 (Ar–*C*), 128.55 (Ar–*C*), 129.51 (Ar–*C*), 133.14 (t, Ar–*C*, $^2J_{CP}$ = 16 Hz), 134.73 (t, Ar–*C*, $^2J_{CP}$ = 16 Hz). ^{31}P{^{1}H} NMR (C_6D_6, 298 K): δ_P 92.3. ^{29}Si{^{1}H} (C_6D_6, 298 K): δ_{Si} −2.34. FTIR ν/cm^{-1} (Nujol): 915 (s), 886 (s), 696 (s), 661 (s), 635 (s), 532 (s), 517 (s), 484 (s) and 454 (s). UV-vis (THF): λ_{max}/cm^{-1} (ε/mol^{-1} cm^{-1}) 15 500 (172), 19 048 (445), 40 486 (19 100). Mössbauer (80 K, mm s^{-1}) I.S. = 0.49, Q.S. = 1.69. CV (298 K, THF, [NBu$_4^n$][[BF$_4$], 1 mM) $E_{1/2}$ = −0.36 V.

5I: III (0.71 g, 1.0 mmol) and $KC_5H_3(^tBu)_2$ (0.22 g, 1.0 mmol), yield: 0.37 g, 49%. Anal. calc'd for $C_{39}H_{45}FeIP_2$: C, 61.76; H, 5.98%. Found: C, 61.65; H, 6.06%. ^{1}H NMR (C_6D_6, 298 K): δ_H 1.29 (s, 18H, CH_3), 2.50 (m, 4H, CH_2), 3.45 (s, 2H, C*H*), 5.38 (s, H, C*H*), 6.95–8.36 (m, 20H, Ar–*H*). ^{13}C{^{1}H} NMR (C_6D_6, 298 K): δ_C 21.20 (*C*Me$_3$), 31.91 (t, *C*H_2 $^1J_{CP}$ = 132 Hz), 62.69 (*C*H), 83.77 (*C*H), 104.20 (*C*^{t}Bu), 127.41 (Ar–*C*), 128.32 (Ar–*C*), 129.09 (Ar–*C*), 133.57 (Ar–*C*), 134.64 (Ar–C), 140.26 (Ar–*C*), 140.57 (Ar–*C*). ^{31}P{^{1}H} NMR (C_6D_6, 298 K): δ_P 80.5. FTIR ν/cm^{-1} (Nujol): 1157 (s), 880 (s), 842 (s), 738 (s), 696 (s), 657 (s), 528 (s), 517 (s), 489 (s) and 467 (s). UV-vis (THF): λ_{max}/cm^{-1} (ε/mol^{-1} cm^{-1}) 14 500 (202), 18 051 (448), 40 323 (210 000). Mössbauer (80 K, mm s^{-1}) I.S. = 0.53, Q.S. = 1.95. CV (298 K, THF, [NBu$_4^n$][[BF$_4$], 1 mM) $E_{1/2}$ = −0.46 V.

General preparative method for 1SIP–5SIP

To a solution of **1Cl–5Cl** in MeCN (10 ml), TMSI (1 : 1 molar ratio) was added dropwise at −30 °C with stirring, the mixture was allowed to warm to room temperature slowly over 18 hours. Volatiles were removed *in vacuo* to yield red solids which were recrystallized from the minimum amount of MeCN with storage at −30 °C to afford red crystals. The crystals were isolated by filtration and dried *in vacuo*.

1SIP: 1Cl (0.46 g, 0.8 mmol) and TMSI (0.12 mL, 0.8 mmol), yield: 0.35 g, 65%. Anal. calc'd for $C_{33}H_{32}FeINP_2$: C, 57.67; H, 4.69; N, 2.04%. Found: C, 57.50; H, 4.78; N, 2.18%. ^{1}H NMR ($CDCl_3$, 298 K): δ_H 0.08 (s, 3H, CH_3), 2.02 (s, 3H, CH_3), 2.18 (m, 4H, CH_2), 4.41 (s, 5H, C_5H_5), 7.31–7.86 (m, 20H, Ar–*H*). ^{13}C{^{1}H}

NMR ($CDCl_3$, 298 K): δ_C 6.25 (CH_3), 28.22 (t, CH_2, $^1J_{CP}$ = 88 Hz), 78.87 (C_5H_5), 129.10 (t, Ar–*C*, $^2J_{CP}$ = 20 Hz), 129.26 (t, Ar–*C*, $^2J_{CP}$ = 18 Hz), 130.48 (Ar–*C*), 130.72 (Ar–*C*), 131.22 (t, Ar–*C*, $^2J_{CP}$ = 20 Hz), 132.72 (t, Ar–*C*, $^2J_{CP}$ = 20 Hz), 134.06 (N≡*C*Me), 136.49 (t, Ar–*C*, $^1J_{CP}$ = 80 Hz), 136.90 (t, Ar–*C*, $^1J_{CP}$ = 80 Hz). $^{31}P\{^1H\}$ NMR ($CDCl_3$, 298 K): δ_P 97.9. FTIR ν/cm^{-1} (Nujol): 2266 (s), 1432 (s), 1175 (s), 1157 (s), 1073 (s), 998 (s), 951 (s), 919 (s), 873 (s), 859 (s), 836 (s), 812 (s), 748 (s), 712 (s), 699 (s), 672 (s), 648 (s), 617 (s), 532 (s), 520 (s), 496 (s) 454 (s), 440 (s) and 429 (s). UV-vis (THF): λ_{max}/cm^{-1} (ε/mol^{-1} cm^{-1}) 16 000 (95.4), 20 202 (392), 24 500 (553), 40 323 (22 900). Mössbauer (80 K, mm s^{-1}) I.S. = 0.39, Q.S. = 2.01. CV (298 K, MeCN, [NBu_4^n][[BF_4], 1 mM) $E_{1/2}$ = 0.26 V.

2SIP: **2Cl** (0.62 g, 1.0 mmol) and TMSI (0.14 mL, 0.8 mmol), yield: 0.57 g, 75%. Anal. calc'd for $C_{38}H_{42}FeINP_2$: C, 60.26; H, 5.59; N, 1.85%. Found: C, 60.36; H, 5.46; N, 1.86%. ^1H NMR ($CDCl_3$, 298 K): δ_H 1.32 (s, 15H, CH_3), 2.17 (s, 3H, CH_3), 2.18 (m, 4H, CH_2) 7.39–7.61 (m, 20H, Ar–*H*). $^{13}C\{^1H\}$ NMR ($CDCl_3$, 298 K): δ_C 7.13 (CH_3), 9.89 (CH_3) 28.57 (t, CH_2, $^1J_{CP}$ = 78 Hz), 87.21 (C_5Me_5), 128.56 (t, Ar–*C*, J_{CP} = 18 Hz), 129.09 (t, Ar–*C*, J_{CP} = 18 Hz), 130.66 (Ar–*C*), 130.87 (Ar–*C*) 132.34 (t, Ar–*C*, J_{CP} = 18 Hz), 133.34 (t, Ar–*C*, J_{CP} = 21 Hz). $^{31}P\{^1H\}$ NMR ($CDCl_3$, 298 K): δ_P 89.9. FTIR ν/cm^{-1} (Nujol): 2248 (s), 1403 (s), 1156 (s), 949 (s), 890 (s), 861 (s), 786 (s), 759 (s), 742 (s), 695 (s), 661 (s), 640 (s), 528 (s), 516 (s), 483 (s) and 456 (s). UV-vis (THF): λ_{max}/cm^{-1} (ε/mol^{-1} cm^{-1}) 15 244 (161), 18 553 (369), 22 750 (810), 40 323 (32 700). Mössbauer (80 K, mm s^{-1}) I.S. = 0.42, Q. S. = 2.00. CV (298 K, MeCN, [NBu_4^n][[BF_4], 1 mM) $E_{1/2}$ = 0.06 V.

3SIP: **3Cl** (1.14 g, 1.8 mmol), and TMSI (0.25 mL, 1.8 mmol), yield: 0.47 g, 36%. Anal. calc'd for $C_{36}H_{40}FeINP_2Si$: C, 56.93; H, 5.31; N, 1.84%. Found: C, 54.54; H, 5.30; N, 2.08%. ^1H NMR ($CDCl_3$, 298 K): δ_H 0.25 (s, 9H, CH_3), 2.03 (s, 3H, CH_3), 2.61 (m, 4H, CH_2), 4.31 (d, 2H, C*H*) 4.85 (s, 2H, C*H*), 7.38–7.86 (m, 20H, Ar–*H*). $^{13}C\{^1H\}$ NMR ($CDCl_3$, 298 K): δ_C −0.53 (CH_3) 6.81 (CH_3), 28.45 (t, CH_2, $^1J_{CP}$ = 80 Hz), 71.06 (*C*H), 72.77 (*C*H), 74.79 (*C*H), 88.29 (*C*H) 129.08 (t, Ar–*C*, $^2J_{CP}$ = 20 Hz), 129.30 (t, Ar–*C*, $^2J_{CP}$ = 20 Hz), 130.70 (Ar–*C*), 130.80 (Ar–*C*), 131.72 (t, Ar–*C*, $^2J_{CP}$ = 20 Hz), 132.72 (t, Ar–*C*, $^2J_{CP}$ = 18 Hz), 134.61 (N*C*Me), 136.24 (t, Ar–*C*, $^1J_{CP}$ = 76 Hz), 136.65 (t, Ar–*C*, $^1J_{CP}$ = 88 Hz). $^{31}P\{^1H\}$ NMR ($CDCl_3$, 298 K): δ_P 95.3. $^{29}Si\{^1H\}$ ($CDCl_3$, 298 K): δ_{Si} −3.12. FTIR ν/cm^{-1} (Nujol): 2268 (s), 1165 (s), 1065 (s) 1031 (s), 950 (s), 899 (s), 871 (s), 832 (s), 746 (s) 698 (s), 674 (s), 616 (s) 527 (s), 517 (s), 490 (s), 455 (s). UV-vis (THF): λ_{max}/cm^{-1} (ε/mol^{-1} cm^{-1}) 20 920 (658), 40 323 (25 300). Mössbauer (80 K, mm s^{-1}) I.S. = 0.39, Q.S. = 1.91. CV (298 K, MeCN, [NBu_4^n][[BF_4], 1 mM) $E_{1/2}$ = 0.25 V.

4SIP: **4Cl** (0.35 g, 0.5 mmol) and TMSI (0.14 mL, 1.0 mmol), yield: 0.27 g, 64%. Anal. calc'd for $C_{39}H_{48}FeINP_2Si_2$: C, 56.32; H, 5.82; N, 1.68%. Found: C, 56.66; H, 5.69; N, 1.63%. ^1H NMR ($CDCl_3$, 298 K): δ_H −0.13 (s, 18H, CH_3), 1.77 (s, 3H, CH_3), 2.51 (m, 4H, CH_2), 4.46 (d, 2H, C*H*) 4.85 (s, 1H, C*H*), 7.46–7.84 (m, 20H, Ar–*H*). $^{13}C\{^1H\}$ NMR ($CDCl_3$, 298 K): δ_C 0.03 (CH_3) 7.79 (CH_3), 29.18 (t, CH_2, $^1J_{CP}$ = 72 Hz), 83.91 (*C*H), 84.41 (*C*H), 98.48 (*C*SiMe$_3$), 129.13 (t, Ar–*C*, $^2J_{CP}$ = 18 Hz), 129.36 (t, Ar–*C*, $^2J_{CP}$ = 18 Hz), 130.77 (Ar–*C*), 130.83 (Ar–*C*) 130.83 (Ar–*C*), 132.36 (t, Ar–*C*, $^2J_{CP}$ = 18 Hz), 133.29 (t, Ar–*C*, $^2J_{CP}$ = 18 Hz), 135.67 (N*C*Me), 136.58 (Ar–*C*). $^{31}P\{^1H\}$ NMR ($CDCl_3$, 298 K): δ_P 89.1. $^{29}Si\{^1H\}$ ($CDCl_3$, 298 K): δ_{Si} −2.76. FTIR ν/cm^{-1} (Nujol): 2273 (s), 1432 (s), 1193 (s), 1178 (s), 1079 (s), 944 (s), 914 (s), 896 (s), 873 (s), 832 (s), 751 (s), 700 (s), 675 (s), 649 (s), 632 (s), 526 (s), 513 (s), 493 (s) and 436 (s). UV-vis (THF): λ_{max}/cm^{-1} (ε/mol^{-1} cm^{-1}) 15 015 (124), 19 120 (392), 23 000 (458), 40 000 (26 700). Mössbauer (80 K, mm s^{-1}) I.S. = 0.44, Q.S. = 1.86. CV (298 K, MeCN, [NBu_4^n][[BF_4], 1 mM) $E_{1/2}$ = 0.26 V.

5SIP: **5Cl** (0.30 g, 1.0 mmol) and TMSI (0.14 Ml, 1.0 mmol), yield: 0.55 g, 69%. Anal. calc'd for $C_{41}H_{48}FeINP_2$: C, 61.59; H, 6.05; N, 1.75%. Found: C, 61.42; H, 5.84; N, 1.73%. ^1H NMR ($CDCl_3$, 298 K): δ_H 0.80 (s, 18H, CH_3), 2.02 (s, 3H, CH_3), 2.18 (m, 4H, CH_2), 4.11 (s, 2H, C*H*), 4.78 (s, 1H, C*H*), 7.28–7.80 (m, 20H, Ar–*H*). $^{13}C\{^1H\}$ NMR ($CDCl_3$, 298 K): δ_C 2.65 (CH_3), 8.29 (CH_3), 31.21 (t, CH_2, $^1J_{CP}$ = 88 Hz), 70.31 (*C*H), 74.89 (*C*H), 109.72 (*C*^{t}Bu), 129.10 (Ar–*C*), 129.35 (Ar–*C*), 130.51 (Ar–*C*), 130.64 (Ar–*C*) 132.29 (Ar–*C*), 133.14 (Ar–*C*), 136.43 (N*C*Me), 137.43 (t, Ar–*C*, J_{CP} = 60 Hz), 137.80 (t, Ar–*C*, J_{CP} = 60 Hz). $^{31}P\{^1H\}$ NMR ($CDCl_3$, 298 K): δ_P 84.6. FTIR ν/cm^{-1} (Nujol): 2267 (s), 1432 (s), 1411 (s), 1364 (s), 1293 (s), 1248 (s) 1179 (s), 1164 (s), 1127 (s), 998 (s), 951 (s), 923 (s), 892 (s), 866 (s), 758 (s), 741 (s), 716 (s), 701 (s), 678 (s), 654 (s), 520 (s), 505 (s), 471 (s) and 438 (s). UV-vis (THF): λ_{max}/cm^{-1} (ε/mol^{-1} cm^{-1}) 14 514 (221), 18 083 (491), 22 500 (716), 40 000 (28 100). Mössbauer (80 K, mm s^{-1}) I.S. = 0.45, Q.S. = 1.97. CV (298 K, MeCN, [NBu_4^n][[BF_4], 1 mM) $E_{1/2}$ = 0.20 V.

General preparative method for 1H–5H

THF (10 ml) was added dropwise to a mixture of **1Cl–2Cl** and $LiAlH_4$ (1 : 5 molar ratio) at −78 °C with stirring, the suspension was allowed to warm to 0 °C and stirred for a further 3 hours. At 0 °C degassed deionised water was added dropwise until the evolution of gas ceased and the volatiles were removed *in vacuo* to yield orange solids which were extracted and recrystallized from hexanes to afford orange crystals. The crystals were collected by filtration and dried *in vacuo*.

1H: **1Cl** (0.56 g, 1.0 mmol) and $LiAlH_4$ (0.19 g, 5.0 mmol), yield: 0.41 g, 73%. ^1H NMR (C_6D_6, 298 K): δ_H −15.94 (t, 1H, Fe*H*, $^2J_{PH}$ = 72 Hz) 1.87 (2H, CH_2), 2.10 (m, 4H, CH_2), 4.31 (s, 5H, C_5H_5), 7.16–7.97 (m, 20H, Ar–*H*). $^{13}C\{^1H\}$ NMR (C_6D_6, 298 K): δ_C 33.02 (t, CH_2, $^1J_{CP}$ = 60 Hz), 75.47 (*C*H), 127.21 (Ar–*C*), 128.48 (Ar–*C*), 133.27 (Ar–*C*), 132.90 (t, Ar–*C*, $^2J_{CP}$ = 40 Hz), 133.27 (t, Ar–*C*, $^2J_{CP}$ = 16 Hz), 133.92 (t, Ar–*C*, $^2J_{CP}$ = 20 Hz), 139.33 (t, Ar–*C*, $^2J_{CP}$ = 36 Hz), 140.11 (t, Ar–*C*, $^2J_{CP}$ = 28 Hz), 141.85 (Ar–*C*), 142.23 (Ar–*C*). $^{31}P\{^1H\}$ NMR (C_6D_6, 298 K): δ_P 111.6. FTIR ν/cm^{-1} (Nujol) 1845 (s), 1621 (w), 1584 (w), 1301 (w), 1260 (w), 1087 (s), 1065 (w), 1027 (w), 812 (w), 740 (w), 695 (vs), 672 (s), 530 (vs), 493 (s), 474 (w) and 439 (w). UV-vis (THF): λ_{max}/cm^{-1} (ε/mol^{-1} cm^{-1}) 39 683 (27 900). Mössbauer (80 K, mm s^{-1}) I.S. = 0.26, Q.S. = 1.91. CV (298 K, THF, [NBu_4^n][[BF_4], 1 mM) $E_{1/2}$ = −0.50 V.

2H: **2Cl** (0.62 g, 1.0 mmol) and $LiAlH_4$ (0.19 g, 5.0 mmol), yield: 0.40 g, 68%. Anal. calc'd for $C_{36}H_{40}FeP_2$: C, 73.22; H, 6.83%. Found: C, 73.34; H, 6.85%. ^1H NMR (C_6D_6, 298 K): δ_H −16.66 (t, 1H, Fe*H*, $^2J_{PH}$ = 80 Hz) 1.73 (15H, CH_3), 1.84 (m, 4H, CH_2), 7.08–7.91 (m, 20H, Ar–*H*). $^{13}C\{^1H\}$ NMR (C_6D_6, 298 K): δ_C

11.35 (CH_3), 33.02 (t, CH_2, $^1J_{CP}$ = 64 Hz) 84.88 (CMe_3), 127.21 (Ar–*C*), 127.43 (Ar–*C*), 132.89 (t, Ar–*C*, $^2J_{CP}$ = 36 Hz), 133.27 (t, Ar–*C*, $^2J_{CP}$ = 16 Hz), 133.92 (t, Ar–*C*, $^2J_{CP}$ = 20 Hz), 138.89 (t, Ar–*C*, $^2J_{CP}$ = 35 Hz), 139.93 (t, Ar–*C*, $^2J_{CP}$ = 32 Hz) 140.11 (t, Ar–*C*, $^2J_{CP}$ = 35 Hz), 141.85 (t, Ar–*C*, $^1J_{CP}$ = 68 Hz), 142.23 (t, Ar–*C*, $^1J_{CP}$ = 68 Hz). $^{31}P\{^1H\}$ NMR (C_6D_6, 298 K): δ_P 107.7. FTIR ν/cm^{-1} (Nujol): 1844 (s), 1153 (s), 1064 (s), 876 (s), 740 (s), 695 (s), 672 (s), 529 (s), 493 (s) and 474 (s). UV-vis (THF): λ_{max}/cm^{-1} (ε/mol^{-1} cm^{-1}) 28 011 (2760), 39 683 (27 900). Mössbauer (80 K, mm s^{-1}) I.S. = 0.25, Q.S. = 1.92. CV (298 K, THF, [NBu$_4^n$][[BF$_4$], 1 mM) E_p^a = −0.67 V, $E_{1/2}$ = −0.71 V.

3H: **3Cl** (1.01 g, 1.5 mmol) and $LiAlH_4$ (0.28 g, 7.5 mmol), yield: 0.31 g, 35%. No satisfactory elemental analysis could be obtained for **3H** due to contamination of samples with free dppe ligand. ^1H NMR (C_6D_6, 298 K): δ_H −15.31 (t, 1H, Fe*H*, $^2J_{PH}$ = 72 Hz), 0.35 (s, 9H, CH_3), 1.92 (m, 4H, CH_2), 4.22 (m, 4H, C*H*), 7.21–7.89 (m, 20H, Ar–*H*). $^{13}C\{^1H\}$ NMR (C_6D_6, 298 K): δ_C 0.34 (CH_3), 31.01 (t, CH_2, $^1J_{CP}$ = 92 Hz), 71.27 (*C*H), 72.91 (*C*H), 80.84 ($CSiMe_3$), 127.69 (Ar–*C*), 128.32 (Ar–*C*), 132.14 (t, Ar–*C*, $^2J_{CP}$ = 16 Hz), 132.82 (t, Ar–*C*, $^2J_{CP}$ = 16 Hz), 143.00 (Ar–*C*), 143.52 (Ar–*C*). $^{31}P\{^1H\}$ NMR (C_6D_6, 298 K): δ_P 110.1. $^{29}Si\{^1H\}$ (C_6D_6, 298 K): δ_{Si} −4.77. FTIR ν/cm^{-1} (Nujol): 1245 (s), 1160 (s), 1066 (s), 1036 (s), 969 (s), 918 (s), 903 (s), 872 (s), 862 (s), 834 (s), 813 (s), 743 (s), 693 (s), 675 (s), 646 (s), 627 (s), 525 (s), 499 (s), 468 (s), 437 (s) and 422 (s). UV-vis (THF): λ_{max}/cm^{-1} (ε/mol^{-1} cm^{-1}) 24 000 (805), 40 161 (8730). Mössbauer (80 K, mm s^{-1}) I.S. = 0.26, Q.S. = 1.70. CV (298 K, THF, [NBu$_4^n$][[BF$_4$], 1 mM) $E_{1/2}$ = −0.50 V.

4H: **4Cl** (1.37 g, 2.0 mmol) and $LiAlH_4$ (0.38 g, 10.0 mmol), yield: 0.54 g, 41%. Anal. calc'd for $C_{37}H_{46}FeP_2$: C, 66.86; H, 6.98%. Found: C, 66.98; H, 7.05%. ^1H NMR (C_6D_6, 298 K): δ_H −16.54 (t, 1H, Fe*H*, $^2J_{PH}$ = 72 Hz), −0.11 (s, 18H, CH_3), 2.60 (m, 4H, CH_2), 4.45 (d, 2H, C*H*), 4.88 (s, 1H, C*H*), 7.49–7.89 (m, 20H, Ar–*H*). $^{13}C\{^1H\}$ NMR (C_6D_6, 298 K): δ_C 0.43 (CH_3), 31.25 (t, CH_2, $^1J_{CP}$ = 88 Hz), 82.16 ($CSiMe_3$), 83.71 (*C*H), 87.01 (*C*H), 127.51 (t, Ar–*C*, $^2J_{CP}$ = 16 Hz), 127.73 (t, Ar–*C*, $^2J_{CP}$ = 16 Hz), 128.40 (Ar–*C*), 128.50 (Ar–*C*), 132.31 (t, Ar–*C*, $^2J_{CP}$ = 18 Hz) 132.77 (t, Ar–*C*, $^2J_{CP}$ = 20 Hz), 146.94 (Ar–*C*). $^{31}P\{^1H\}$ NMR (C_6D_6, 298 K): δ_p 104.8. $^{29}Si\{^1H\}$ (C_6D_6, 298 K): δ_{Si} −5.01. FTIR ν/cm^{-1} (Nujol): 1245 (s), 1184 (s), 1155 (s), 1074 (s), 968 (s), 924 (s), 911 (s), 864 (s), 832 (s), 742 (s), 696 (s), 669 (s), 634 (s), 522 (s), 494 (s), 479 (s), 444 (s) and 427 (s). UV-vis (THF): λ_{max}/cm^{-1} (ε/mol^{-1} cm^{-1}) 24 096 (1660), 39 683 (14 200). Mössbauer (80 K, mm s^{-1}) I.S. = 0.28, Q.S. = 1.71. CV (298 K, THF, [NBu$_4^n$][[BF$_4$], 1 mM) $E_{1/2}$ = −0.53 V.

5H: **5Cl** (0.63 g, 1.0 mmol) and $LiAlH_4$ (0.19 g, 5.0 mmol), yield: 0.46 g, 53%. Anal. calc'd for $C_{39}H_{46}FeP_2$: C, 74.05; H, 7.33%. Found: C, 72.03; H, 7.15%. ^1H NMR (C_6D_6, 298 K): δ_H −15.65 (t, 1H, Fe*H*, $^2J_{PH}$ = 84 Hz) 1.19 (s, 18H, CH_3), 1.98 (m, 4H, CH_2), 4.05 (d, 2H, C*H*), 4.09 (s, 1H, C*H*), 7.17–8.02 (m, 20H, Ar–*H*). $^{13}C\{^1H\}$ NMR (C_6D_6, 298 K): δ_C 22.54 (CMe_3), 30.72 (CH_3), 32.06 (CH_2) 69.93 (*C*H), 71.17 (*C*H), 108.73 (C^tBu), 127.46 (Ar–*C*), 127.66 (Ar–*C*), 128.20 (Ar–*C*), 128.26 (Ar–*C*), 132.26 (t, Ar–*C*, $^2J_{CP}$ = 24 Hz) 132.65 (t, Ar–*C*, $^2J_{CP}$ = 16 Hz), 144.19 (Ar–*C*), 144.39 (Ar–*C*). $^{31}P\{^1H\}$ NMR (C_6D_6, 298 K): δ_P 104.5. FTIR ν/cm^{-1} (Nujol): 1431 (s), 1360 (s), 1198 (s), 1162 (s), 1047 (2), 939 (s), 918 (s), 911 (s), 874 (s), 842 (s), 743 (s), 696 (s), 676 (s), 657 (s), 617 (s), 588 (s), 524 (s), 514 (s), 496 (s) and 475 (s). UV-vis (THF): λ_{max}/cm^{-1} (ε/mol^{-1} cm^{-1}) 23 474 (2610), 39 683 (20 500). Mössbauer (80 K, mm s^{-1}) I.S. = 0.27, Q.S. = 1.96. CV (298 K, THF, [NBu$_4^n$][[BF$_4$], 1 mM) $E_{1/2}$ = −0.62 V.

X-ray crystallographic details

Crystallographic data can be found in the ESI in cif format.† Crystals were examined variously on: (a) a Bruker AXS CCD area detector diffractometer operating at 90 K/150 K using graphite-monochromated Mo Kα radiation (λ = 0.71073 Å), with intensities integrated from a sphere of data recorded on 0.3° frames by rotation of ω, or (b) an Oxford Diffraction CCD area detector diffractometer operating at 90 K using mirror-monochromated Cu Kα radiation (λ = 1.5418 Å) with intensities integrated from a sphere of data recorded on 1° frames by rotation of $\acute{\omega}$. Cell parameters were refined from the observed positions of all strong reflections in the data set. The structures were solved by either direct methods or heavy atom method and refined by least-squares methods on all unique F^2 values, with all non-H non solvent atoms being anisotropic. The largest residual electron densities in final difference syntheses were close to heavy atoms unless stated otherwise. Absorption correction was performed by multi-scan methods. Criterion for observed reflections is $I > 2\sigma(I)$ and weighting scheme used is $W = 1/[\sigma^2(F_o^2) + (xP)^2 + yP]$ where $P = (F_o^2 + 2F_c^2)/3$. Programs used for Bruker AXS were SMART (control), SAINT (integration) and SHELXTL for structure solution and refinement. Programs used for Oxford diffraction were CrysalisPro CCD (control), CrysalisPro RED (integration), SHELXTL for structure solution and refinement.[56]

Cyclic voltammetry experimental details and ESI†

Electrochemical measurements were performed using an Autolab PGSTAT20 potentiostat with a three-electrode configuration consisting of a saturated calomel electrode (SCE) reference electrode, Pt wire secondary electrode and a glassy carbon working electrode. All voltammograms were recorded at ambient temperatures for solutions of the sample at *ca.* 1 mM in tetrahydrofuran (THF) or acetonitrile (MeCN) containing 0.5 M or 0.1 M [NBu$^n_4$][BF$_4$], respectively, as the supporting electrolyte. Samples were prepared in a glove box and maintained under an argon atmosphere using Schlenk line techniques during the experiment. All electrochemical potentials were measured relative to SCE and were corrected for liquid-junction potentials *via* the use of the $[(\eta^5\text{-}C_5H_5)_2Fe]^+/[(\eta^5\text{-}C_5H_5)_2Fe]$ ($[Cp_2Fe]^+/[Cp_2Fe]$) couple as an internal redox standard. When the potential of a redox process of the compound of interest overlapped with that of the $[Cp_2Fe]^+/[Cp_2Fe]$ couple, either the $[(\eta^5\text{-}Me_5)_2Fe]^+/[(\eta^5\text{-}C_5Me_5)_2Fe]$ or $[Cp_2Co]^+/[Cp_2Co]$ couples was used as a standard. Under these circumstances, the redox processes of the compound were referenced to the $[Cp_2Fe]^+/[Cp_2Fe]$ couple by an independent calibration under identical conditions; $E_{1/2}$ $[Cp_2Co]^+/[Cp_2Co]$ was −1.358 V *vs.* $[Cp_2Fe]^+/[Cp_2Fe]$ in THF at 1 V s^{-1} (used for **4H** only) and

$E_{1/2}$ $[(\eta^5\text{-}C_5Me_5)_2Fe]^+/[(\eta^5\text{-}C_5Me_5)_2Fe]$ was −0.505 V *vs.* $[Cp_2Fe]^+/[Cp_2Fe]$ in MeCN at 0.1 V s^{-1} (used for **1SIP–5SIP**).

DFT experimental and ESI†

Restricted gas-phase DFT calculations were performed using the Amsterdam Density Functional (ADF) suite version 2012.01 with initial models of were derived from the X-ray crystal structures of **1Cl–5Cl**, **1Br–5Br**, **1I–5I**, **1SIP–5SIP** and **1H–5H**.[57–59] The DFT calculations employed a Slater-type orbital (STO) all-electron triple-ζ-plus one polarization function basis set from the ZORA/TZP database of the ADF suite for all atoms. The scalar relativistic (SR) approach was used within the ZORA Hamiltonian for the inclusion of relativistic effects. The calculations employed the local density approximation (LDA) with the correlation potential due to Vosko *et al.*[60] Gradient corrections were performed using the functionals of Becke[61] and Perdew.[62] Pictorial representations of the MOs were generated using MOLEKEL[63] and the orbital compositions were calculated using AOMIX.[64]

Acknowledgements

We thank the Royal Society, EPSRC, ERC, and University of Nottingham for supporting this work.

References

1 R. D. Theys, M. E. Dudley and M. M. Hossain, *Coord. Chem. Rev.*, 2009, **253**, 180.
2 A search of the Cambridge Strucutral Database v1.17, accessed on 15–01–2015, reveals over six hundred complexes containing a $CpFe(CO)_2$ fragment bonded to a d- or f-block metal.
3 M. P. Blake, N. Kaltsoyannis and P. Mountford, *Chem. Commun.*, 2013, **49**, 3315; B. Oelkers, M. V. Butovskii and R. Kempe, *Chem. – Eur. J.*, 2012, **18**, 13566; S. T. Liddle and D. P. Mills, *Dalton Trans.*, 2009, 5569; S. T. Liddle, *Philos. Trans. R. Soc. London, Ser A*, 2009, **465**, 1673; P. Beletskaya, A. Z. Voskoboynikov, E. B. Chuklanova, N. I. Kirillova, A. K. Shestakova, I. N. Parshina, A. I. Gusev and G. K.-I. Magomedov, *J. Am. Chem. Soc.*, 1993, **115**, 3156.
4 B. M. Gardner, J. McMaster, F. Moro, W. Lewis, A. J. Blake and S. T. Liddle, *Chem. – Eur. J.*, 2011, **17**, 6909; B. M. Gardner, W. Lewis, A. J. Blake and S. T. Liddle, *Inorg. Chem.*, 2011, **50**, 9631; D. Patel, D. M. King, B. M. Gardner, J. McMaster, W. Lewis, A. J. Blake and S. T. Liddle, *Chem. Commun.*, 2011, **47**, 295; S. T. Liddle, D. P. Mills, B. M. Gardner, J. McMaster, C. Jones and W. D. Woodul, *Inorg. Chem.*, 2009, **48**, 3520; B. M. Gardner, J. McMaster, W. Lewis and S. T. Liddle, *Chem. Commun.*, 2009, 2851; S. T. Liddle, J. McMaster, D. P. Mills, A. J. Blake, C. Jones and W. D. Woodul, *Angew. Chem., Int. Ed.*, 2009, **48**, 1077.
5 A. P. Sobaczynski, T. Bauer and R. Kempe, *Organometallics*, 2013, **32**, 1363.
6 B. M. Gardner, D. Patel, A. D. Cornish, J. McMaster, W. Lewis, A. J. Blake and S. T. Liddle, *Chem. – Eur. J.*, 2011, **17**, 11266.
7 M. J. Mays and P. L. Sears, *J. Chem. Soc., Dalton Trans.*, 1973, 1873; G. Hata, H. Kondo and A. Miyake, *J. Am. Chem. Soc.*, 1968, **90**(9), 2278–2281; J. E. Barclay, G. J. Leigh, A. Houlton and J. Silver, *J. Chem. Soc., Dalton Trans.*, 1988, 2865–2870; S. Pohl, U. Opitz, D. Hasse and W. Saak, *Z. Anorg. Allg. Chem.*, 1995, **621**, 1140–1146; R. Langer, F. Bönisch, L. Maser, C. Pietzonka, L. Vondung and T. P. Zimmermann, *Eur. J. Inorg. Chem.*, 2015, 141–148.
8 J. Niemeyer, D. A. Addy, I. Riddlestone, M. Kelly, A. L. Thompson, D. Vidovic and S. Aldridge, *Angew. Chem., Int. Ed.*, 2011, **50**, 8908; J. A. van Rijn, E. Gouré, M. A. Siegler, A. L. Spek, E. Drent and E. Bouwman, *J. Organomet. Chem.*, 2011, **696**, 1899; S. G. Davies, *J. Organomet. Chem.*, 1979, **179**, C5.
9 E. C. Fitzgerald, A. Ladjarafi, N. J. Brown, D. Collison, K. Costuas, R. Edge, J.-F. Halet, F. Justaud, P. J. Low, H. Meghezzi, T. Roisnel, M. W. Whiteley and C. Lapinte, *Organometallics*, 2011, **30**, 4180; Y. Tanaka, J. A. Shaw-Taberlet, F. D. R. Justaud, O. Cador, T. Roisnel, M. Akita, J.-R. Hamon and C. Lapinte, *Organometallics*, 2009, **28**, 4656; L. Medei, L. Orian, O. V. Semeikin, M. G. Peterleitner, N. A. Ustynyuk, S. Santi, C. Durante, A. Ricci and C. Lo Sterzo, *Eur. J. Inorg. Chem.*, 2006, 2582; M. I. Bruce, K. Costuas, T. Davin, B. G. Ellis, J.-F. Halet, C. Lapinte, P. J. Low, M. E. Smith, B. W. Skelton, L. Toupet and A. H. White, *Organometallics*, 2005, **24**, 3864; F. de Montigny, G. Argouarch, K. Costuas, J.-F. Halet, T. Roisnel, L. Toupet and C. Lapinte, *Organometallics*, 2005, **24**, 4558; N. Le Narvor and C. Lapinte, *C. R. l'Académie. Sci., Ser. IIC Chem.*, 1998, **1**, 745; T. Weyland, C. Lapinte, G. Frapper, M. J. Calhorda, J.-F. Halet and L. Toupet, *Organometallics*, 1997, **16**, 2024; F. Coat and C. Lapinte, *Organometallics*, 1996, **15**, 477; N. Le Narvor and C. Lapinte, *Organometallics*, 1995, **14**, 634.
10 D. Patel, F. Moro, J. McMaster, W. Lewis, A. J. Blake and S. T. Liddle, *Angew. Chem., Int. Ed.*, 2011, **50**, 10388.
11 S. El-Tarhuni, M. Ho, M. H. Kawser, S. Shi and M. W. Whiteley, *J. Organomet. Chem.*, 2014, **752**, 30.
12 P. Hamon, L. Toupet, J.-R. Hamon and C. Lapinte, *Organometallics*, 1996, **15**, 10.
13 M. J. Mays and P. L. Sears, *J. Chem. Soc., Dalton Trans.*, 1973, 1873.
14 C. Roger, P. Hamon, L. Toupet, H. Rabaa, J. Y. Saillard, J. R. Hamon and C. Lapinte, *Organometallics*, 1991, **10**, 1045; Y.-P. Ou, D. Feng and J.-J. Yuan, *Acta Crystallogr., Sect. E: Struct. Rep. Online*, 2010, **66**, m921.
15 D. H. Hill, M. Parvez and A. Sen, *Acta Crystallogr., Sect. C: Cryst. Struct. Commun.*, 1990, **46**, 133.
16 As determined by a search of the Cambridge Structural Database v1.17, accessed on the 15-01-2015.
17 J.-R. Hamon, P. Hamon, L. Toupet, K. Costuas and J.-Y. Saillard, *C. R. Chim.*, 2002, **5**, 89.

18 M. Jimenez-Tenorio, M. C. Puerta and P. Valerga, *Organometallics*, 1994, **13**, 3330.
19 E. B. Lobkovskii, M. Y. Antipin, A. P. Borisov, V. D. Makhaev, K. N. Semenenko and Y. T. Struchkov, *Koord. Khim.*, 1980, **6**, 1267.
20 R. H. Morris, J. F. Sawyer, M. Shiralian and J. Zubkowski, *J. Am. Chem. Soc.*, 1985, **107**, 5581.
21 M. Knorr, J. Mueller and U. Schubert, *Chem. Ber.*, 1987, **120**, 879.
22 J. S. Ricci, T. F. Koetzle, M. T. Bautista, T. M. Hofstede, R. H. Morris and J. F. Sawyer, *J. Am. Chem. Soc.*, 1989, **111**, 8823.
23 P. B. Hitchcock, M. A. N. D. A. Lemos, M. F. Meidine, J. F. Nixon and A. J. L. Pombeiro, *J. Organomet. Chem.*, 1991, **402**, C23.
24 M. F. Meidine, M. A. N. D. A. Lemos, A. J. L. Pombeiro, J. F. Nixon and P. B. Hitchcock, *J. Chem. Soc., Dalton Trans.*, 1998, 3319.
25 J.-G. Lee, G.-S. Jung and S. W. Lee, *Bull. Korean Chem. Soc.*, 1998, **19**, 267.
26 S. S. P. R. Almeida, M. F. C. G. da Silva, J. J. R. Fraustoda Silva and A. J. L. Pombeiro, *J. Chem. Soc., Dalton Trans.*, 1999, 467.
27 J. G. Lee, B. S. Yoo, N. S. Choi, K. I. Park, S. I. Cho, C. Lee and S. W. Lee, *J. Organomet. Chem.*, 1999, **589**, 138.
28 L. M. D. R. S. Martins, J. J. R. Frausto Da Silva, A. J. L. Pombeiro, R. A. Henderson, D. J. Evans, F. Benetollo, G. Bombieri and R. A. Michelin, *Inorg. Chim. Acta*, 1999, **291**, 39.
29 J. Y. Baeg, W. S. Han and S. W. Lee, *J. Korean Chem. Soc.*, 2002, **46**, 427.
30 B.-S. Yoo, N.-S. Choi, C. Y. Shim, Y. Son and S. W. Lee, *Inorg. Chim. Acta*, 2000, **309**, 137.
31 J. H. Lee, B. S. Yoo and S. W. Lee, *Inorg. Chim. Acta*, 2001, **321**, 75.
32 S. S. P. R. Almeida, M. F. C. Guedes da Silva, L. B. Jerzykiewicz, P. Sobota and A. J. L. Pombeiro, *Inorg. Chim. Acta*, 2003, **356**, 259.
33 H. V. Nanishankar, M. Nethaji and B. R. Jagirdar, *Indian J. Chem., Sect. A: Inorg., Bio-inorg., Phys., Theor. Anal. Chem.*, 2003, **42A**, 2332.
34 M. P. Rabalo, A. P. S. Teixeira, M. H. Garcia, M. F. Minas da Piedade, M. T. Duarte, A. R. Dias, J. Campo, W. Wenseleers and E. Goovaerts, *Eur. J. Inorg. Chem.*, 2006, 2175.
35 J. G. Cordaro, D. Stein and H. Gruetzmacher, *J. Am. Chem. Soc.*, 2006, **128**, 14962.
36 C. Hansch, A. Leo and R. W. Taft, *Chem. Rev.*, 1991, **91**, 165.
37 G. Boschloo and A. Hagfeldt, *Acc. Chem. Res.*, 2009, **42**, 1819.
38 M. Tilset, I. Fjeldahl, J.-R. Hamon, P. Hamon, L. Toupet, J.-Y. Saillard, K. Costuas and A. Haynes, *J. Am. Chem. Soc.*, 2001, **123**, 9984.
39 F. Paul and C. Lapinte, *Coord. Chem. Rev.*, 1998, **178–180**, 431.
40 N. N. Greenwood and T. C. Gibb, *Mössbauer Spectroscopy*, Chapman and Hall Ltd, London, 1971.
41 V. Guillaume, P. Thominot, F. Coat, A. Mari and C. Lapinte, *J. Organomet. Chem.*, 1998, **565**, 75.
42 P. Hamon, L. Toupet, J. R. Hamon and C. Lapinte, *Organometallics*, 1992, **11**, 1429.
43 T. A. Albright, J. K. Burdett and M.-H. Wangbo, *Orbital Interactions in Chemistry*, John Wiley, New York, 1985.
44 G. M. Aston, S. Badriya, R. D. Farley, R. W. Grime, S. J. Ledger, F. E. Mabbs, E. J. L. McInnes, H. W. Morris, A. Ricalton, C. C. Rowlands, K. Wagner and M. W. Whiteley, *J. Chem. Soc., Dalton Trans.*, 1999, 4379.
45 I. M. Bartlett, S. Carlton, N. G. Connelly, D. J. Harding, O. D. Hayward, A. G. Orpen, C. D. Ray and P. H. Reiger, *Chem. Commun.*, 1999, 2403.
46 S. T. Krueger, R. Poli, A. L. Rheingold and D. L. Staley, *Inorg. Chem.*, 1989, **28**, 4599.
47 T. C. Zietlow, M. D. Hopkins and H. B. Gray, *J. Am. Chem. Soc.*, 1986, **108**, 8266.
48 T. Hascall, D. Rabinovich, V. J. Murphy, M. D. Beachy, R. A. Friesner and G. Parkin, *J. Am. Chem. Soc.*, 1999, **121**, 11402.
49 S. T. Krueger, B. E. Owens and R. Poli, *Inorg. Chem.*, 1990, **29**, 2001.
50 C. M. Fendrick, L. D. Schertz, E. A. Mintz, T. J. Marks, T. E. Bitterwolf, P. A. Horine, T. L. Hubler, J. A. Sheldon and D. D. Belin, *Inorg. Synth.*, 1992, **29**, 193.
51 F. X. Kohl and P. Jutzi, *J. Organomet. Chem.*, 1983, **243**, 119.
52 H. Schumann, I. Albrecht, J. Loebel, E. Hahn, M. B. Hossain and D. Van der Helm, *Organometallics*, 1986, **5**, 1296.
53 C. Ting, J.-C. Tsai, Y.-C. Chen, S.-S. Hua, T.-T. Su and Y.-S. Chao, *Pat. No* US6207773B1, 2001, Metallocene catalyst for preparing olefin polymer.
54 M. D. Walter, C. D. Sofield, C. H. Booth and R. A. Andersen, *Organometallics*, 2009, **28**, 2005.
55 D. J. Evans, P. B. Hitchcock, G. J. Leigh, B. K. Nicholson, A. C. Niedwieski, F. S. Nunes and J. F. Soares, *Inorg. Chim. Acta*, 2001, **319**, 147.
56 Bruker SMART and SAINT Bruker AXS Inc., Madison, Wisconsin, 2001; G. M. Sheldrick, *SHELXTL, version 5*, Bruker AXS Inc., Madison, WI; *SHELXTL, version 5*, Bruker AXS Inc., Madison, WI, 2001.
57 G. t. Velde, F. M. Bickelhaupt, S. J. A. v. Gisbergen, C. F. Guerra, E. J. Baerends and S. J. G. Ziegler, *J. Comput. Chem.*, 2001, **22**, 931.
58 C. F. Guerra, J. G. Snijders, G. t. Velde and E. J. Baerends, *Theor. Chem. Acc.*, 1998, **99**, 391.
59 *ADF2014, Theoretical Chemistry*, Vrije Universiteit, Amsterdam, The Netherlands, http://www.scm.com.
60 S. H. Vosko, L. Wilk and M. Nusair, *Can. J. Phys.*, 1980, **58**, 1200.
61 A. D. Becke, *Phys. Rev. A*, 1988, **38**, 3098.
62 J. P. Perdew, *Phys. Rev. B: Condens. Matter*, 1986, **33**, 8822.
63 S. Portmann and H. P. Lüthi, *Chimia*, 2000, **54**, 766.
64 S. I. Gorelsky and A. B. P. Lever, *J. Organomet. Chem.*, 2001, **635**, 187.